Quaternary Science Reviews 339 (2024) 108850

Contents lists available at ScienceDirect

Quaternary Science Reviews

journal homepage: www.elsevier.com/locate/quascirev

Holocene rangeland characteristics on the northeastern Tibetan Plateau in relation to climate and pastoralism from sedimentary ancient DNA

Ying Liu [a,b], Kathleen R. Stoof-Leichsenring [a], Bernhard Diekmann [a,b], Ulrike Herzschuh [a,b,c,*]

[a] Alfred Wegener Institute Helmholtz Centre for Polar and Marine Research, Polar Terrestrial Environmental Systems, Telegrafenberg, 14473, Potsdam, Germany
[b] Institute of Environmental Science and Geography, University of Potsdam, 14476, Potsdam, Germany
[c] Institute of Biology and Biochemistry, University of Potsdam, Potsdam, 14476, Germany

ARTICLE INFO

Handling editor: P Rioual

Keywords:
Sedimentary ancient DNA (sedaDNA)
Northeast Tibetan plateau
Paleovegetation reconstruction
Human activity
Pastoralism
Biodiversity

ABSTRACT

The northeast Tibetan Plateau, functioning as an alpine pasture, has been influenced by prehistoric settlements for millennia. However, the extent to which climate and anthropogenic activities have shaped this rangeland remains contentious. Here, we present sedimentary ancient DNA evidence from Lake Donggi Cona sediment core, focusing on the *trn*L p6-loop region of vascular plants and the internal transcribed spacer (ITS1) region of nuclear ribosomal DNA for Poaceae and Cyperaceae. Our findings indicate that before 7.4 cal ka BP, the rangeland was characterized by alpine steppe with low richness, influenced by dry environmental conditions. By 7.4 cal ka BP, more taxa migrated to the study region, with a relatively high richness supported by a humid environment. The climate conditions, coupled with low grazing pressure, sustained a relatively high pastoral quality. Intensified nomadic activities after 4 cal ka BP contributed to a severe decline in pasture quality, characterized by a high abundance of poisonous taxa. This study highlights that both human activity and moisture availability contribute to the rangeland characteristic, with human activity as the predominant factor since 4 cal ka BP.

1. Introduction

Containing one of the world's largest alpine grassland areas, the Tibetan Plateau is covered by alpine grassland across 54–70% of its total area (Y. Wang et al., 2022c). However, the extent to which the alpine grassland ecosystem is shaped by climate factors or anthropogenic land use is still contentious (Chen et al., 2020; Miehe et al., 2014). Specifically, the region is experiencing pronounced warming amplification within the context of global climate change (C. Zhang et al., 2023a), and anthropogenic activities, primarily livestock grazing, are severely degrading the grassland (Bardgett et al., 2021). Insights from the past, as provided by paleoecological records, can help to disentangle the drivers, enhancing our ability to forecast future changes, as well as to identify potential conservation or restoration targets.

The northeastern Tibetan Plateau, which served as a crucial corridor for the prehistoric colonization of the inner Tibetan Plateau (Chen et al., 2015), stands out as one of the most threatened regions by grassland degradation (S. Wang et al., 2022b). Several fossil pollen studies have been conducted in this region, and spatial heterogeneity in the vegetation exists (Herzschuh et al., 2009; N. Wang et al., 2022a; Wang et al., 2023; Wei et al., 2020; Wischnewski et al., 2011; Zhao et al., 2007). Generally, forest areas in the surrounding mountains started to extend since the early Holocene and reached a maximum value in the middle Holocene (Cheng et al., 2013; Shen et al., 2005; J. Zhang et al., 2023b), which was explained as the consequence of precipitation changes in response to the East Asia Summer Monsoon. In the boundary of alpine meadow and steppe, the ratio of *Artemisia*/Cyperaceae (A/Cy) decreased, especially after the middle Holocene, which indicated the vegetation shifted to Cyperaceae dominated alpine meadows. However, it is still unclear whether the vegetation shift resulted from a wetter environment or anthropogenic activities (Herzschuh et al., 2011; Miehe et al., 2014).

Although the earliest human activities (Denisovans) on the northeastern Tibetan Plateau (NETP) date back to the late Middle Pleistocene (Chen et al., 2019; Zhang et al., 2020), a limited impact is suggested by the scarcity of archaeological sites (Wang et al., 2020; Zhang et al., 2022). At approximately 4 cal ka BP, crops and domestic animals were introduced into the Hexi Corridor to the north of the Plateau (Dong et al., 2018), which facilitated extensive and permanent human settlement in the higher elevation areas of the NETP after 3.6 cal ka BP (Chen

* Corresponding author. Alfred Wegener Institute Helmholtz Centre for Polar and Marine Research, Polar Terrestrial Environmental Systems, Telegrafenberg, 14473, Potsdam, Germany.
E-mail address: Ulrike.Herzschuh@awi.de (U. Herzschuh).

https://doi.org/10.1016/j.quascirev.2024.108850
Received 2 May 2024; Received in revised form 13 July 2024; Accepted 17 July 2024
Available online 24 July 2024

et al., 2015), potentially altering the local environment. Several species, such as *Saussurea* spp., *Potentilla anserina*, and the poisonous weed *Stellera* spp. have been used as grazing indicators (Kramer et al., 2010; Miehe et al., 2014). Additionally, *Kobresia pygmaea* (syn. *Carex parvula*), endemic to High Asia, is a dominant component of the alpine meadow. Its presence suggests a human-influenced landscape, as evidenced by its complete disappearance or sparse occurrence upon grazing exclosure (Miehe et al., 2014). Yet, identifying the Cyperaceae taxa to the species level in palynological records is challenging, due to the limited taxonomic resolution of pollen analysis. Similarly, while human activity on the Tibetan Plateau is thought to affect plant diversity (Liu et al., 2023; Lu et al., 2017), limited taxonomic resolution hampers plant richness estimation from paleoecological records (Goring et al., 2013; Gosling et al., 2018).

Sedimentary ancient DNA (sedaDNA) provides a higher taxonomic resolution than palynology, especially for herbaceous plants (Liu et al., 2021; Pedersen et al., 2013; Rijal et al., 2021). It has been employed to assess plant diversity in response to alpine habitat loss (Liu et al., 2021), and to evaluate turnover in terrestrial and aquatic ecosystems associated with cryosphere loss on the Tibetan Plateau (Liu et al., 2024). Moreover, research related to DNA preservation has been conducted on the Tibetan Plateau (Jia et al., 2022). Employing the g/h plant metabarcoding method, which targets the vascular plant *trn*L p6-loop locus of the chloroplast genome (Taberlet et al., 2007), can help improve plant richness reconstructions. However, limited resolution of the g/h primer for Poaceae and Cyperaceae hampers a detailed analysis of grassland composition. Application of the first internal transcribed spacer (ITS1) of nuclear ribosomal DNA for Poaceae and Cyperaceae (Ait Baamrane et al., 2012; Willerslev et al., 2014) supports a more detailed plant composition reconstruction. Additionally, the high taxonomic resolution of sedaDNA enhances detection of anthropogenic-related taxa signals (Garcés-Pastor et al., 2022), thereby facilitating the assessment of plant composition responses to human-induced activities.

In this study, we reconstruct the rangeland characteristics around Lake Donggi Cona on the northeast Tibetan Plateau over the past 12,000 years. Using the g/h metabarcoding method, along with the ITS1

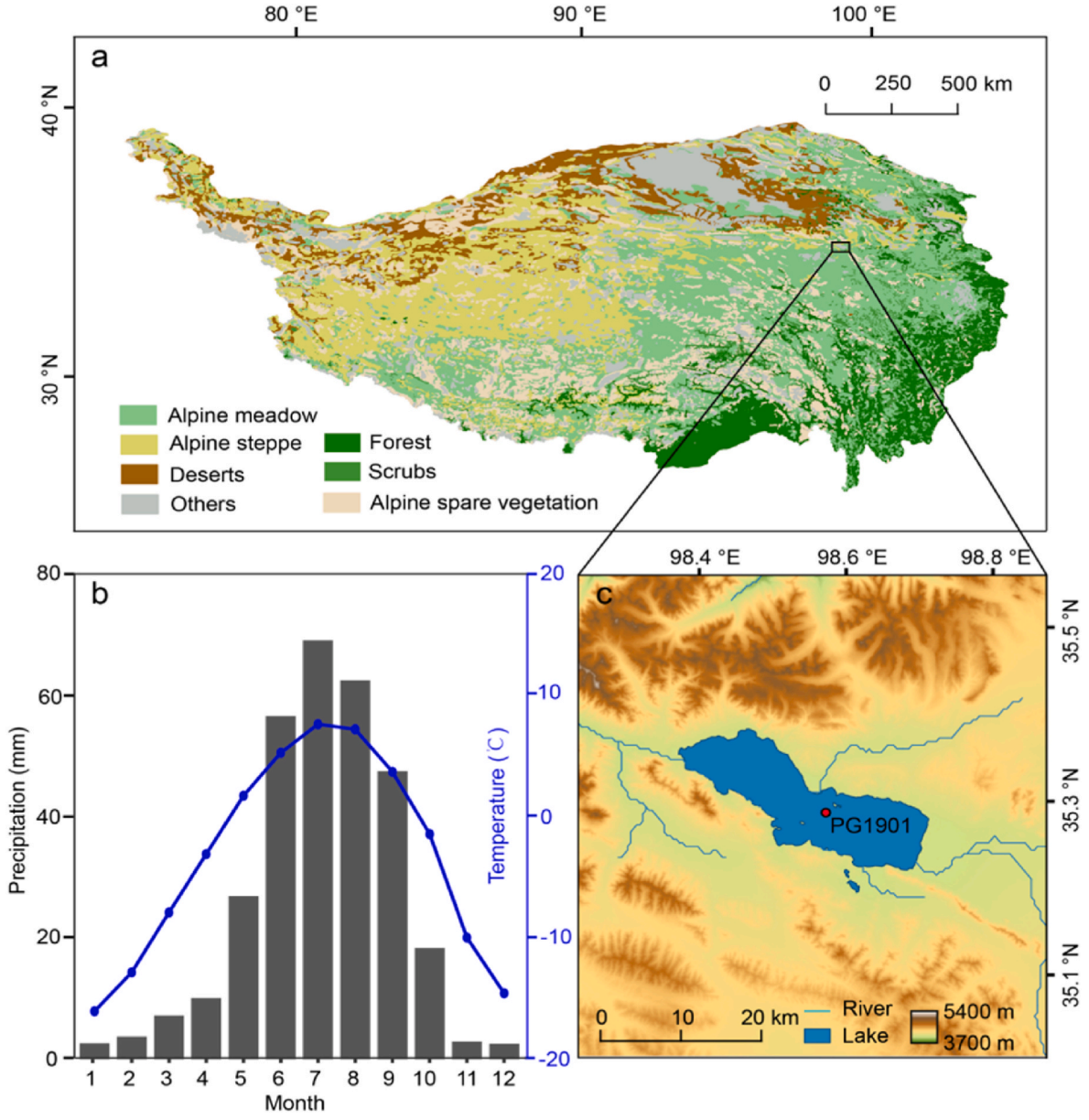

Fig. 1. Location, modern vegetation type, climate, and geomorphological settings of the study region. a: Location of the lake region and vegetation type of the Tibetan Plateau; b: Meteorological data between 1950 and 1990 CE from the Madoi station (Wang et al., 2014); c: Location of the PG1901 coring site.

metabarcoding method specific to Poaceae and Cyperaceae, we assessed changes in plant composition and richness. Subsequently, the results were compared with regional vegetation dynamics, climate-change patterns, and archaeological records. Our objectives are: (1) to explore how plant composition turnover responds to climate change on the northeast Tibetan Plateau; (2) to determine how prehistorical human activity shaped the rangeland characteristic; and (3) to examine how climate and human activity influence changes in plant richness in the study region.

2. Materials and methods

2.1. Study area and sample collection

Lake Donggi Cona (98.55208° E, 35.28217° N; 4090 m a.s.l.) is located on the northeastern Tibetan Plateau in Qinghai Province, China, near Amne Machin in the eastern Kunlun mountain range (Dietze et al., 2010; Opitz et al., 2016) (Fig. 1a). The lake fills a tectonic pull-apart basin on the Kunlun Fault (Yan et al., 2021), covering an area of about 230 km^2, with a catchment of 3174 km^2. The northern catchment area comprises dissected Early and Middle Triassic limestones and sandstones faulted against Triassic quartzite and black to green shales, overlaid by reddish Neogene conglomerates and sandstones. In the south, the basin is enclosed by an elevated, elongated mountain ridge composed of Middle Permian limestone. The catchment area is characterized by steep relief gradients in the north and southeast, while lower mountains with gently sloping inclines define the southern and northeastern regions (Dietze et al., 2010; Mischke et al., 2010b). The maximum water depth is 98 m (measured in summer 2006), and the lake receives a constant flow from the east through a perennial river, the Dong Qu, supplemented by episodic inflows from the north. The lake's outflow is regulated by a gauge station established in the 1970s CE, directing water into the Tuosu River (Dietze et al., 2010; Wang et al., 2014). The local monsoonal climate conditions are characterized by relatively cold and dry winters and relatively wet summers, with a mean annual air temperature of −3.1 °C. The local mean temperatures in January and July are −15.9 °C and 7.8 °C, respectively (Fig. 1b). The mean annual precipitation is 311 mm, of which 76% falls during the monsoon season (Wang et al., 2014).

As the lake is in the transition zone between alpine steppe and alpine meadow, the vicinity of the lake hosts alpine steppe vegetation dominated by Poaceae, *Kobresia* (Cyperaceae), and *Artemisia*. The Amne Machin mountain range sustains alpine meadows, dominated by *Kobresia* spp., and interspersed with patches of alpine shrubs (*Salix*) alongside *Saussurea* spp. and *Potentilla* spp. (Wang et al., 2014; Wang and Herzschuh, 2011). Human impact on the lake is limited to the grazing of yaks and sheep in its vicinity, as well as the modification of its outflow through straightening (Mischke et al., 2010a).

A 5.75 m long sediment core (PG1901) from the central part of the lake (35.27863°N, 98.56206°E) (Fig. 1c), was recovered in spring 2008 (Opitz et al., 2012). The coring site is in the central part of the lake at 40 m water depth. The core was transported to and stored in the Alfred Wegener Institute for Polar and Marine Research (AWI) in Potsdam, Germany. A reservoir effect of 2290 ± 35 years was determined from the top sample of the PG1901 dating result and confirmed by other cores from the same lake (Opitz et al., 2012). In this study, ^{14}C dating was performed on the total organic carbon content of 15 bulk sediment samples using accelerator mass spectrometry (AMS) at the MICADAS (Mini Carbon Dating System) Laboratory of AWI in Bremerhaven, Germany. All results are listed in Table 1. These adjusted ^{14}C ages were calibrated using the 'IntCal 20' Radiocarbon Calibration Curve (Reimer et al., 2020) with the IntCal package (Heaton et al., 2020), and the age-depth model established using a Bayesian approach with the 'rbacon' package in R (Blaauw and Christen, 2011) (Fig. 2). The new age-depth model reveals a sedimentation rate pattern similar to previous findings. Specifically, the bottom two lithological units (LU4 and LU5) exhibit a relatively moderate sedimentation rate of 48.33 cm/ka. In contrast, lithological unit 3 (LU3) shows a high sedimentation rate of 69.61 cm/ka, while the upper two lithological units (LU1 and LU2) have a relatively low sedimentation rate of 22.17 cm/ka. The lithology, sediment composition change, and the reason for the sedimentary rate variation of the core have been described in detail by Opitz et al. (2012). Based on the new age-depth model, the bottommost sample is dated to 17,000 cal yr BP. Two outliers were detected, located at the boundaries of lithological units (Fig. 2), which may be attributed to the influence of mixed samples from different lithological units. Only samples younger than 12,000 cal yr BP were used for the DNA extraction.

Table 1
Accelerator mass spectrometry radiocarbon dates for core PG1901 of Lake Donggi Cona (TOC = total organic carbon).

Lab. no	Depth (cm)	Material	^{14}C age (yr BP)	Two sigma error (±)	Reservoir corrected (yr BP)
9240.1.1	11	TOC	3,105	52	757
9241.1.1	96	TOC	5,924	52	3,576
9242.1.1	110	TOC	6,446	53	4,098
9243.1.1	131	TOC	7,414	53	5,066
9244.1.1	149	TOC	8,435	53	6,087
9245.1.1	167	TOC	8,600	53	6,252
9246.1.1	191	TOC	9,541	54	7,193
9247.1.1	209	TOC	10,395	54	8,047
9248.1.1	225	TOC	11,262	55	8,914
9249.1.1	237	TOC	12,169	56	9,821
9250.1.1	306	TOC	13,643	41	11,295
9251.1.1	405	TOC	13,069	40	10,721
9252.1.1	450	TOC	14,774	43	12,426
9253.1.1	496	TOC	18,007	55	15,659
9254.1.1	556	TOC	16,180	50	13,832

2.2. DNA extraction and amplification

The subsampling of the sediment core PG1901 was conducted in a clean climate chamber of the Helmholtz Centre Potsdam-German Research Centre for Geosciences (GFZ) at a room temperature of 4 °C. The risk of contamination with modern DNA was reduced by covering up personal clothing and using sterile subsampling equipment. The sediment core was cut into two halves and subsampling of the central, undisturbed sediments of the working-half was conducted by scraping the surface layer of the halved core with a sterile scalpel and extracting a slice. Parts of the sediment slice that touched the core liner were removed. The clean sediment samples of about 2–10 g of sediment were stored at −20 °C in sterile tubes until further use. In total, 39 sediment samples of the Holocene period were collected.

DNA extractions of the 39 sediment samples were performed in the dedicated paleogenetic laboratory at the Alfred Wegener Institute, Helmholtz Centre for Polar and Marine Research, Potsdam, Germany. Each extraction batch included nine sediment samples plus one extraction control and followed the modified protocol of the DNeasy PowerSoilMax Soil Kit (Qiagen, Germany). The samples were added to a mixture of 1.2 mL of C1 buffer, 0.4 mL of 2 mg/mL Proteinase K (VWR International, Germany), and 0.5 mL of 1 M dithiothreitol (VWR International, Germany) in PowerBead tubes, and vortexed for 30 s at maximum speed. Then, the samples were homogenized for 50 s using the MP Biomedicals™ FastPrep™-24 Bead-Beating device at maximum speed and incubated at 56 °C in a rocking shaker overnight. Subsequent steps followed the instructions of the manufacturer Qiagen. Final DNA extracts were eluted in 2 mL C6 buffer, where 1 mL was concentrated using the GeneJET PCR Purification Kit (Thermo Fisher Scientific) using 50 μL elution buffer. The purified DNA concentration was measured using the ds-DNA BR Assay Kits and the Qubit® 2.0 fluorometer (Invitrogen, USA). Then, the DNA solution was diluted to 3 ng/μL for the subsequent PCR process.

PCR reactions were performed using the g

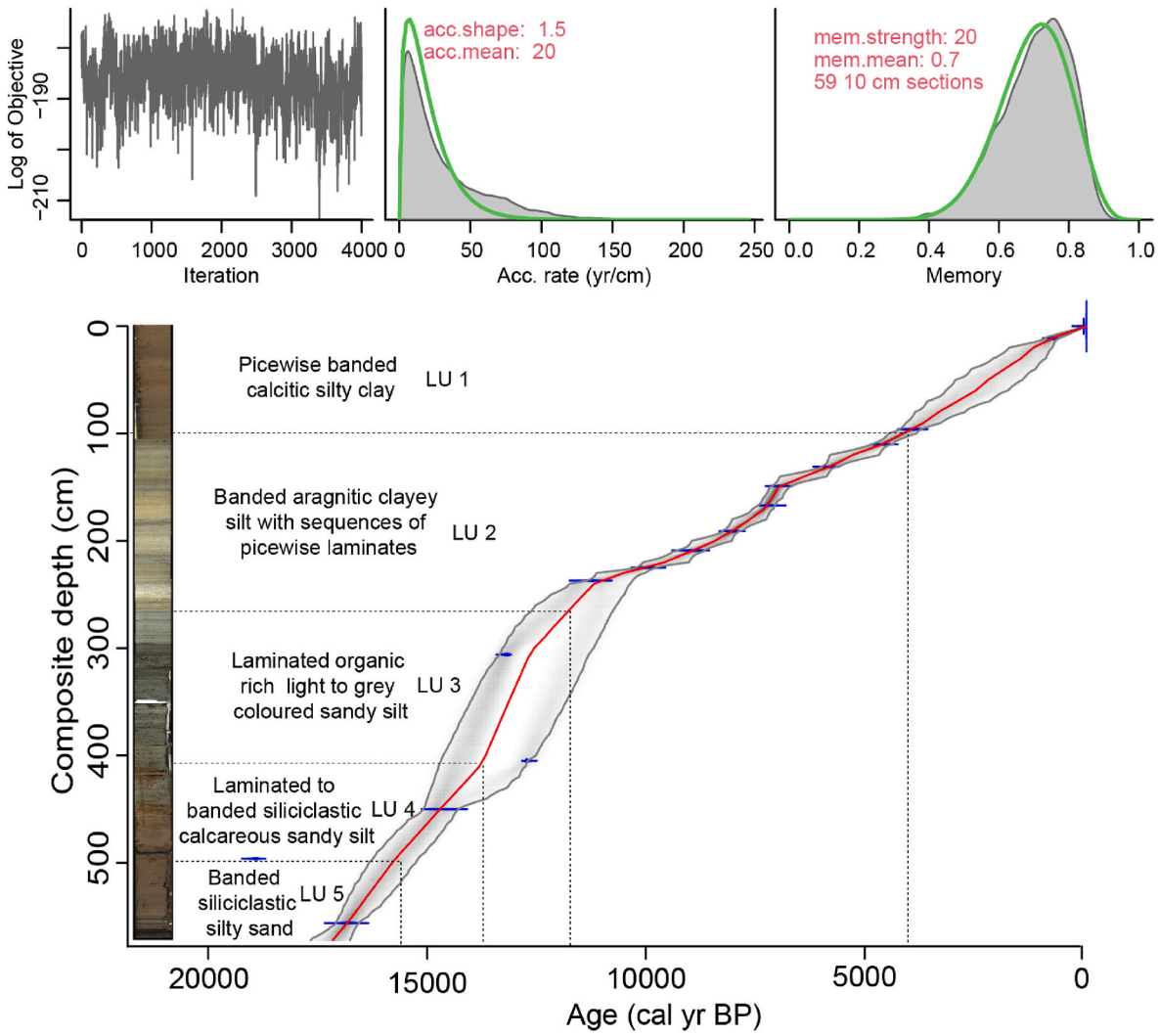

Fig. 2. Age-depth model of the PG1901 core from Lake Donggi Cona.

(GGGCAATCCTGAGCCAA) and h (CCATTGAGTCTCTGCACCTATC) primers targeting the vascular plant *trn*L p6-loop locus of the chloroplast genome (Taberlet et al., 2007). A second plant barcode, specifically targeting the plant families Poaceae and Cyperaceae, was applied to increase the taxonomic resolution of dominant taxa in the study region. This metabarcode encompasses the internal transcribed spacer (ITS1) of nuclear ribosomal DNA. For Poaceae ITS1-F, GATATCCGTTGCCGAGAGTC and ITS1Poa-R, CCGAAGGCGTCAAGGAACAC (Ait Baamrane et al., 2012) were used, and for Cyperaceae ITS1-F, GATATCCGTTGCCGAGAGTC and ITS1Cyp-R, GGATGACGCCAAGGAACAC (Willerslev et al., 2014) were employed. All primers were tagged with an NNN-8bp tag at the 5' end, which allowed indexing of the PCR samples and subsequent demultiplexing (Valentini et al., 2009). PCR reactions for the *trn*L p6-loop were conducted in a final volume of 25 μL, using 3 μL of DNA extract diluted to 3 ng/μL as template, and 12.8 μL H_2O, 2.5 μL Taq DNA Polymerase PCR Puffer (10×), 0.25 mM dNTPS, 0.8 mg Bovine Serum Albumin, 2 mM $MgSO_4$ (Invitrogen, USA), 1 U Platinum® Taq High Fidelity DNA Polymerase (Invitrogen, USA), and 0.2 mM of each primer. PCRs were run with initial denaturation at 94 °C for 5 min, followed by 40 cycles of 94 °C for 30 s, 50 °C (annealing temperature) for 30 s, 68 °C (elongation temperature) for 30 s, and a final extension at 72 °C for 10 min. Similar PCR conditions were used for PCR reactions for the ITS1 metabarcode except for the annealing temperature, which was set to 55 °C. An extraction control (blank) and one no-template control (NTC) were included in each PCR batch to identify possible contamination during extraction and PCR set-up. The PCR success was checked using gel electrophoresis on 2% agarose gels (Carl Roth GmbH & Co. KG, Germany). Finally, three positive PCR replicates for each sediment sample were aggregated and purified using the MinElute PCR Purification Kit (Qiagen, Germany), following the recommended protocol, and finally eluted in 30 μL of elution buffer. Concentrations of PCR products were measured with the ds-DNA BR Assay and the Qubit® 2.0 fluorometer (Invitrogen, USA) using 1 μL of PCR product and all purified PCR products were equimolarly pooled to a final volume of 30 μL with a concentration of 30 ng/μL. Pools of *trn*L p6-loop (APMG-58) and ITS1 (APMG-65) PCR products were sequenced on a NextSeq Illumina sequencing device with NextSeq Mid Kit and 2 × 150bp paired-end mode at the company Fasteris Genesupport SA, Switzerland. Sequencing of APMG-58 and APMG-65 resulted in 7497 Mb (Megabases) and 12,378 Mb, respectively.

2.3. Bioinformatic analyses

The raw sequencing data were analyzed using the OBITools software (version 3.0.0) (Boyer et al., 2016). First, forward and reverse sequences were merged and filtered for high quality reads using the obi *alignpairedend* function. Then, sequences were demultiplexed using the obi *ngsfilter* and deduplicated with obi *uniq*. After that, PCR or sequencing errors were removed using obi *clean* and obi *ecotag* was applied for taxonomic assignment against an OBITools database. Specific OBITools

databases were built for the *trn*L p6-loop, ITS1-Poaceae, and ITS1-Cyperacae. The *trn*L p6-loop database was built by using the Arctic and Boreal vascular plant and bryophyte reference libraries (Soininen et al., 2015; Sønstebø et al., 2010; Willerslev et al., 2014) and EMBL Nucleotide Database (standard sequence release 143). The metabarcode specific EMBL database was constructed with an in silico PCR (Bellemain et al., 2010; Ficetola et al., 2010) using the g/h primers allowing for five mismatches between the primers and the targeted sequences of the EMBL entries. For *trn*L, the taxonomic assignment involves referencing the two separate databases, with taxonomic determination based on an identity value. For the ITS1 databases, the same in silico PCR approach was applied.

2.4. Data quality control

After taxonomic assignment, only *trn*L amplicon sequence variants (ASVs) with a 100% identity match to the reference database were retained. For the ITS data, ASVs with more than 98% identity match to the reference database were kept. To check the quality of the PCR replicates, the compositional data at the ASV level were transformed using the "Hellinger" method (decostand() function). Afterwards, the similarity of the three PCR samples was evaluated using non-metric multidimensional scaling (NMDS) (metaMDS() function in R package vegan v. 2.6–4 (Oksanen et al., 2022)). Where replicates of the same sample show a pronounced distance from all other samples – indicating low-quality replicates – the PCR sample was excluded. In addition, if the replicates of the same sample did not form a cluster, distinct compositions were assumed and the corresponding PCR samples were excluded.

2.5. Statistical analyses

The number of archaeological sites for each 500-year time bin was determined from a dataset comprising 139 prehistoric sites in the northeast Tibetan Plateau (Cao and Dong, 2020). A moisture index, created from a synthesis of northeastern Tibetan Plateau effective moisture records (Wu et al., 2023), was interpolated to the same age as the sedaDNA samples using the 'approx' function in R.

Detrended correspondence analysis (DCA) (Hill and Gauch, 1980) was run to calculate the gradient length of the plant compositional data, which, as it was less than 3 standard deviations (SD), made an assumption of linear relationships in our data appropriate. Redundancy analysis (RDA) was conducted using the rda function in the R vegan package (version 2.6–4) (Oksanen et al., 2022). It ordinated the plant compositional data across all samples under the constraints of the effective moisture index of the northeastern Tibetan Plateau (Wu et al., 2023) and human activity (represented by numbers of archaeological sites (Cao and Dong, 2020)). Poaceae and Cyperaceae taxa were fitted to the RDA plot using the 'envfit' function. The adjusted R^2 of the RDA was partitioned using the varpart function in the vegan package to assess the explanatory capacity of each driver.

The richness was determined by the total number of taxa types, indicated by the corresponding Amplicon sequence variant (ASV) types. As taxonomic richness increases with read counts, richness was calculated based on rarefied read counts (base count = 61,099 for the g/h data, base count = 130,292 for the ITS1 Poaceae data, and base count = 61,595 for the ITS1 Cyperaceae data) for each sample using the R iNEXT package (Chao et al., 2014). Zonation of the plants was based on a stratigraphically constrained cluster analysis (CONISS; Grimm, 1987) and plant richness of all g/h plant metabarcoding data.

To evaluate the potential drivers of plant richness, a generalized additive model (GAM) was run with plant richness as the response variable, and human activity and effective moisture index as the explanatory variables using the gam function in the R mgcv package (Wood, 2011).

3. Results

3.1. SedaDNA record based on g/h metabarcoding since the early Holocene

After filtering, a total of 3,152,600 terrestrial seed-plant sequence reads amplified using the g/h primer were assigned to 235 taxa with 100% identity. We divided the sedaDNA record into three main zones (Fig. 3). During the period from 12 to 7.4 cal ka BP, the sedaDNA spectra are dominated by Salicaceae (*Salix*), Rosaceae (*Potentilla*, *Comarum*), Asteraceae, and Poaceae, sporadically, together with *Ephedra*. Taxa richness has stable low values. Between 7.4 and 5 cal ka BP, the percentage of Salicaceae increases, and plant richness displays a sharp increase as well. After 5 cal ka BP, although Salicaceae abundance decreases compared to the previous period, it remains dominant. Furthermore, Rosaceae abundance declines, while Polygonaceae (*Knorringia*, *Rheum*, *Bistorta vivipara*), Asteraceae (*Artemisia*, *Saussurea*), Crassulaceae (*Rhodiola*), Saxifragaceae (*Saxifraga*), and Boraginaceae (*Microula filicaulis*) all exhibit an increase in abundance. Taxa richness is high, peaking at 3 cal ka BP.

The RDA revealed that effective moisture (Wu et al., 2023) and human activity (Cao and Dong, 2020) together explain 10.0% ($p < 0.05$) of the total variance in the sedaDNA g/h assemblages (Fig. 4). Variation partitioning indicates that only 1.2% of the variance can be uniquely explained by effective moisture ($p = 0.161$) while human activity explains 2.3% ($p = 0.001$), but most is explained by them jointly (Fig. 5).

3.2. ITS1 Poaceae primer-targeted sedaDNA record since the early Holocene

A total of 5,006,659 ASV reads were captured from 35 samples amplified using the ITS1 primer, with a median of 130,292 ASV reads per sample. Taking a >98% identity threshold, 119 ASVs were assigned to Poaceae. During the period from 12 to 7.4 cal ka BP, the Poaceae spectra are dominated by *Lolium* and the tribe Poeae, mainly consisting of *Poa* and *Dactylis glomerata* (Fig. 6). Between 7.4 and 5 cal ka BP, the Poeae and Stipeae taxa dominate. Notably, *Puccinellia tenuiflora* and *Stipa* abundance increases clearly compared to the previous period, while *Poa* and *Lolium* disappear. After 5 cal ka BP, *Poa* and *Lolium* reappear, and the abundance of *Festuca*, *Poa,* and *Deschampsia* increase. The richness is stable and around 100 for the whole Holocene period.

3.3. ITS1 Cyperaceae primer-targeted sedaDNA record since the early Holocene

A total of 2,872,297 sequence reads were amplified using the ITS1 primer and assigned to 19 Cyperaceae taxa with a >98% identity. During the period from 12 to 7.4 cal ka BP, the Cyperaceae spectra are dominated by *Carex myosuroides*, *C. stenantha*, *C.* subgen *Vignea,* and *C. borealipolaris*. The Cyperaceae taxa richness is relatively low during this period (Fig. 7). After 7.4 cal ka BP, *Carex borealipolaris* has high values and taxa richness increases. Subsequently, there is an increase in *Kobresia pygmaea* abundance, which dominates the Cyperaceae assemblage, alongside *Carex* subgen *Vignea* and *C. borealipolaris*. Cyperaceae richness is relatively high during this period.

4. Discussion

4.1. Holocene vegetation responses to climate change on the northeast Tibetan Plateau

Comparing plant reconstruction results from sedaDNA and pollen, sedaDNA detected more local plant taxa, while the pollen identified more regional plants but had limitations in plant richness reconstruction (Figs. 3 and 8, Supplementary Fig. 1). Both methods detected minor tree taxa signals, consistent with the absence of arboreal plants in the region

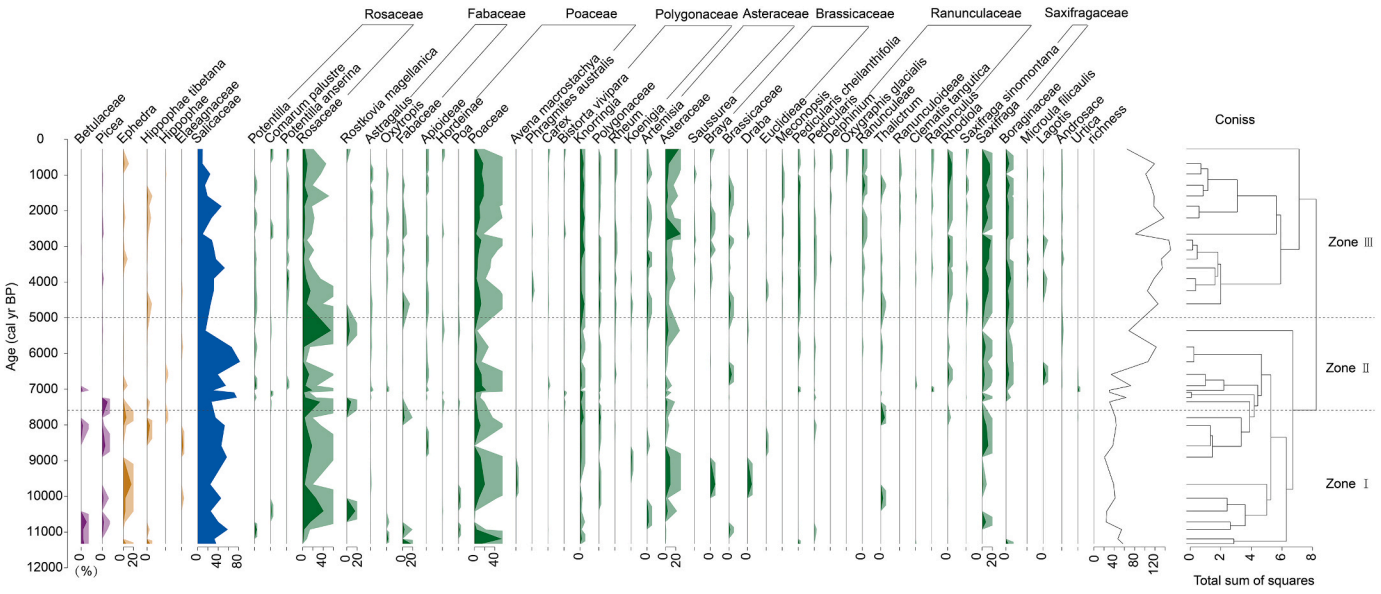

Fig. 3. Composition of plant taxa (relative abundance in %) and richness of plant taxa with total abundance more than 2% over the past 12 kyr in Lake Donggi Cona based on g/h plant metabarcoding. Zonation based on CONISS clustering and richness change is shown in the right panel.

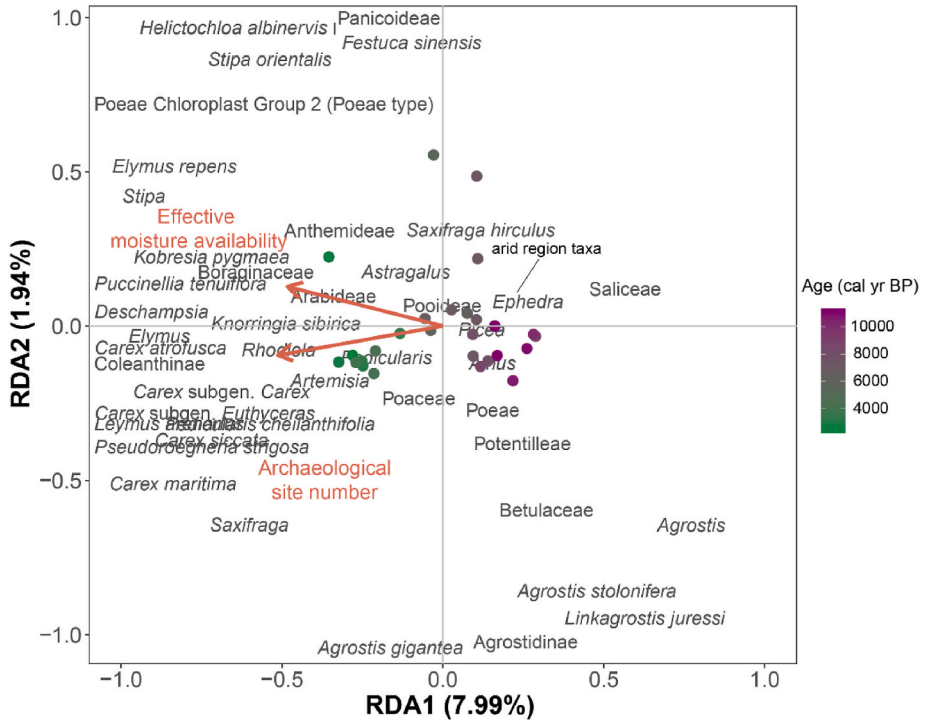

Fig. 4. Redundancy analysis (RDA) biplot of the plant compositional data based on g/h primer metabarcoding constrained by archaeological site number or effective moisture index, representing potential drivers of the compositional change. Only taxa exhibiting scores above 0.1 on either RDA axis1 or axis2 are shown.

(Wang et al., 2014), the sporadic presence of Betulaceae and *Picea* DNA signals may derive from long-distance transferred pollen. For shrub taxa, pollen indicated a low abundance, primarily consisting of *Ephedra*. In contrast, sedaDNA detected higher shrub abundance, predominantly corresponding to Salicaceae taxa, which grow along the lakeshore. Additionally, pollen data showed more signals of Chenopodiaceae, common in desert environments and possibly transferred from the surrounding alpine desert, while sedaDNA detected minimal signals of this taxon. These findings support that pollen captures more regional plant taxa signals, whereas sedaDNA identifies more local taxa. Furthermore, sedaDNA detected more taxa than pollen, supporting plant richness reconstruction.

Between 11.4 and 7.4 cal ka BP, the Lake Donggi Cona area was characterized by Poaceae-*Carex* alpine steppe landscapes with low richness (Fig. 3). The vegetation was dominated by taxa from Poaceae (*Poa*, *Lolium*), *Carex*, Asteraceae (*Artemisia*), and Rosaceae (*Potentilla*). The presence of *Ephedra* suggests a drought-adapted characteristic of the local vegetation. Likewise, pollen analysis from the same lake shows a relatively high *Ephedra* abundance at this time (Wang et al., 2014), and low pollen concentration (N. Wang et al., 2022a). Additionally,

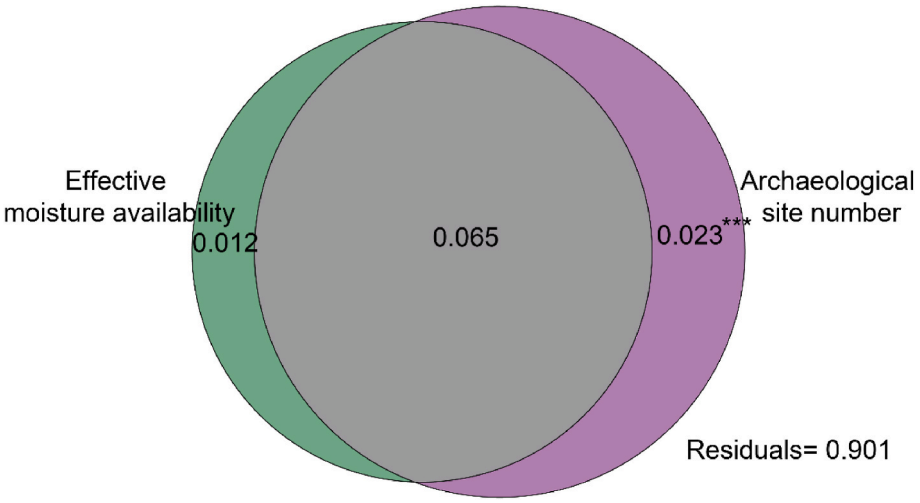

Fig. 5. Partitioning of the proportion of variance explained by archaeological site number and effective moisture index in g/h primer metabarcoding of plant assemblages. Only the unique variance of archaeological site number is significant (p = 0.001).

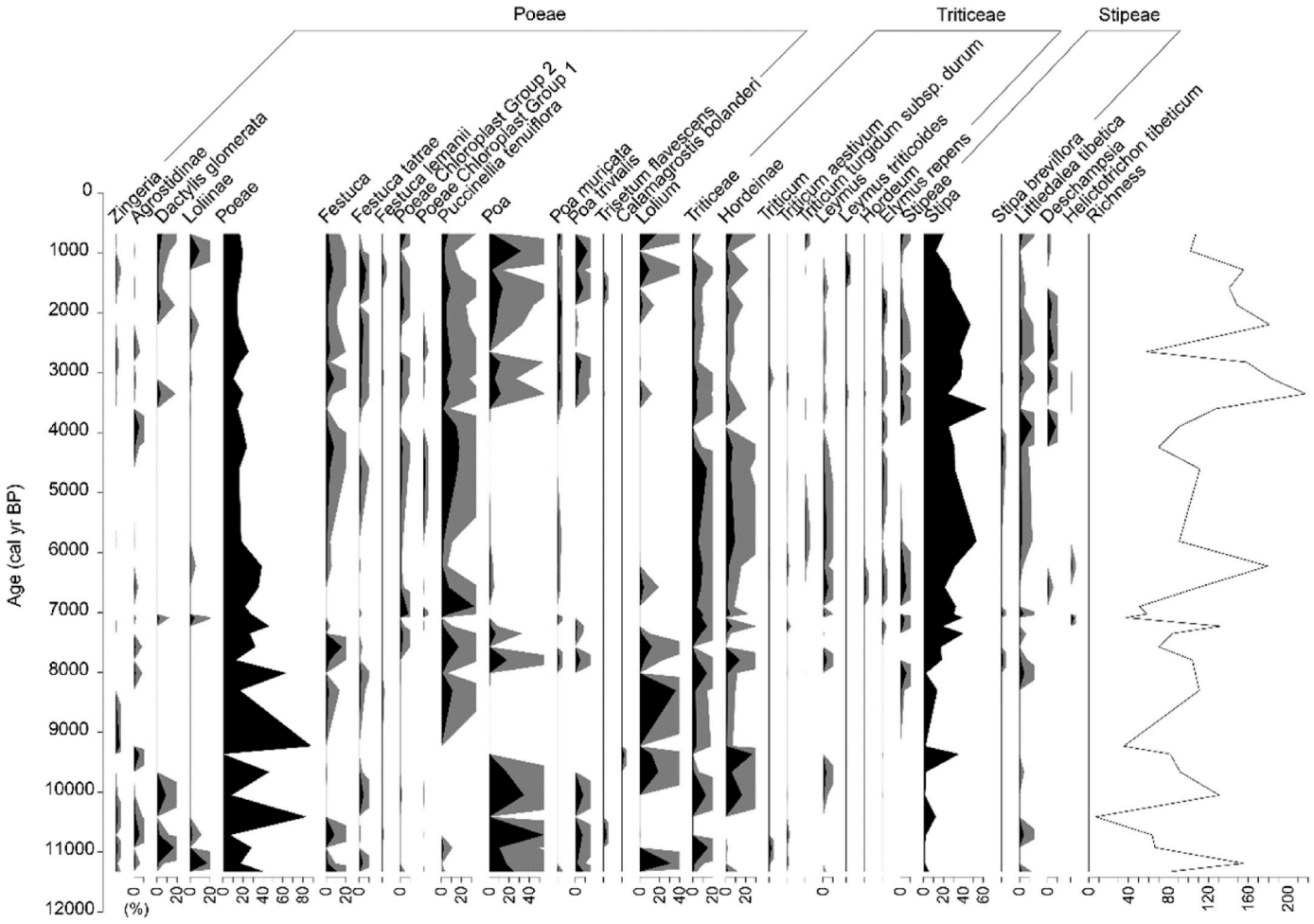

Fig. 6. Composition of the Poaceae family (relative abundance in %) and richness where total abundance is more than 2% over the past 12 kyr in Lake Donggi Cona based on results from ITS metabarcoding.

pollen-based vegetation reconstructions from Lake Donggi Cona, Lake Kuhai, and Lake Koucha all revealed a relatively high *Artemisia* to Cyperaceae ratio (A/Cy) (Herzschuh et al., 2009; Wischnewski et al., 2011) (Fig. 9g, h,9i). All of this vegetation evidence supports an inference of dry climate conditions dominating the region. Additionally, total organic carbon isotopes ($\delta^{13}C$) (Liu et al., 2013) of Lake Qinghai (Fig. 9a), the OH-GDGTs inferred lake level of Lake Dalianhai (Wu et al., 2020) (Fig. 9b), and the isotope synthesis of the northeast Tibetan Plateau (Wu et al., 2022) (Fig. 9c) all indicate a low lake level during this period. Despite debates about the increased aeolian deposition at this

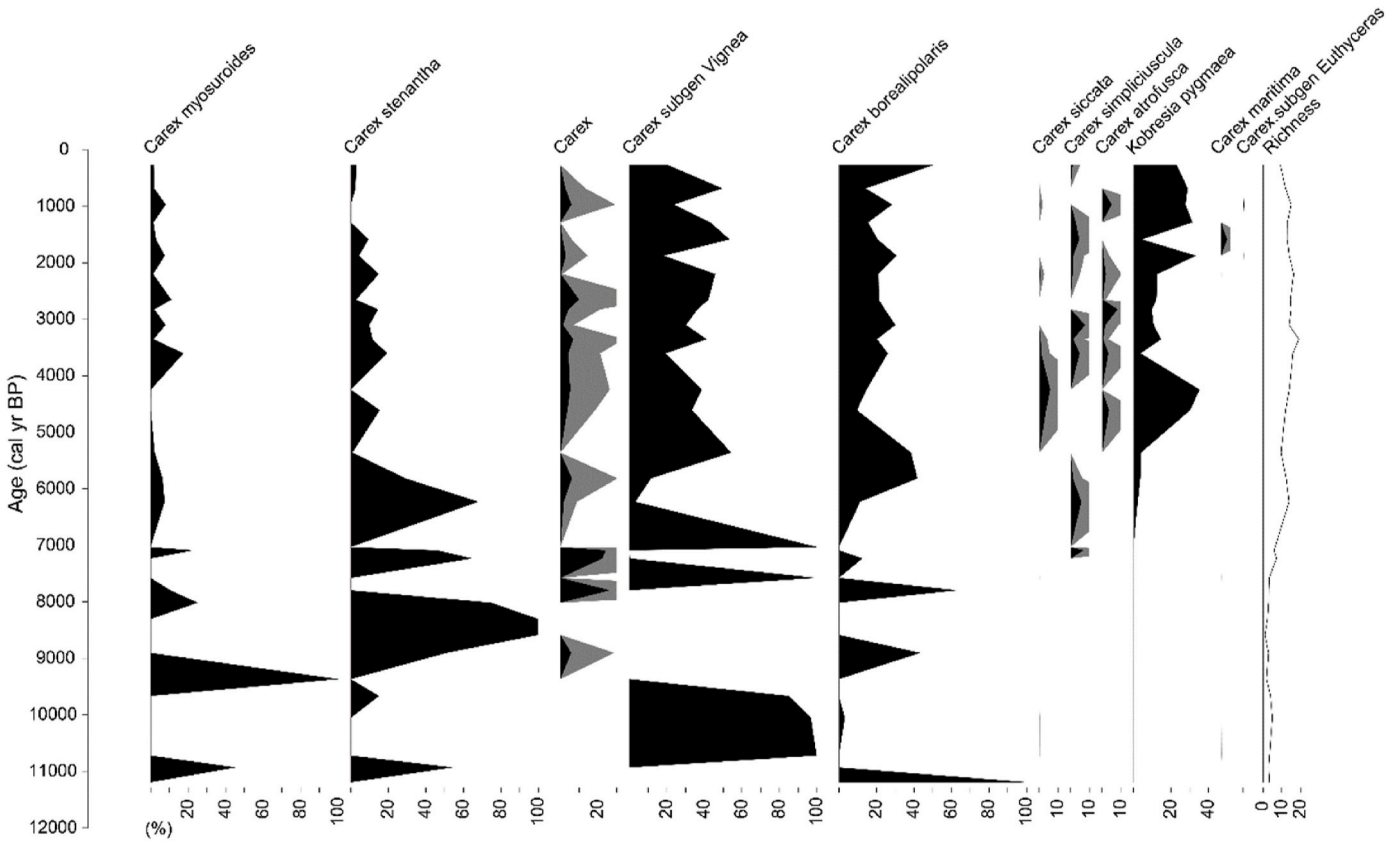

Fig. 7. Composition of the Cyperaceae family (relative abundance in %) and richness where total abundance is more than 2% over the past 12 kyr in Lake Donggi Cona based on results from ITS metabarcoding.

time, which have been attributed to either arid conditions or vegetation retention (Fig. 9e) (Chen et al., 2016; Stauch et al., 2012), the presence of *Ephedra* in our study, coupled with desert conditions, confirms an arid environment during the early Holocene.

However, divergent proxy signals of climate change have been detected on the northeast Tibetan Plateau. For example, the lake level reconstructions of Lake Donggi Cona indicate higher levels during the early Holocene (Dietze et al., 2013), which appears to contradict the vegetation signals. As indicated by the authors, this lake level rise may have been driven by the Asian monsoon, which contributed to higher precipitation during the early Holocene. Additionally, the lake level was influenced by melting glaciers, thawing permafrost, and increased fluvial activity, as well as active tectonic and geomorphological dynamics. Thus, the lake level of Lake Donggi Cona was controlled by both climatic and non-climatic factors. In contrast, our vegetation record represents the effective moisture of the study region, reflecting the combined signal of temperature and precipitation. During the early Holocene, high precipitation may have been offset by high evaporation (consistent with the saline environment of Lake Donggi Cona (Mischke et al., 2010a)) in the semi-arid region, resulting in less effective moisture (Herzschuh, 2006; Qiang et al., 2016). Coincidentally, the conflict between the high stand of Lake Genggahai and the low vegetation cover is reconciled by this explanation (Li et al., 2021).

Between 7.4 and 5 cal ka BP, the study region was characterized by alpine steppe, with an increase in plant richness. The vegetation was dominated by taxa from Poaceae (*Stipa*, *Puccinellia*), *Carex*, and new occurrences of various forb taxa, while *Ephedra* is rarely detected (Fig. 3). The samples post 7.4 cal ka BP mainly align along the negative end of RDA axis 1, with ITS Cyperaceae significantly correlated with this axis (Fig. 4). This observation suggests a relatively humid environment during this period in the Lake Donggi Cona region. However, the pollen analysis from Lake Donggi Cona reveals a relatively high *Artemisia* to Cyperaceae ratio (A/Cy), which may reflect differences in the representational ranges of sedaDNA and pollen. Situated in the transitional zone among alpine desert, alpine steppe, and alpine meadow, the pollen data from Lake Donggi Cona reflect the complex regional signal. Although Donggi Cona reached its second maximum level around 7.5 cal ka BP and freshwater conditions established during this period (Dietze et al., 2013; Mischke et al., 2010a), this was possibly related to non-climatic factors. However, the regional lake level and moisture reconstructions generally suggest a high lake level and effective moisture (Fig. 9a, c, 9d, 9e). Overall, the high moisture availability on the northeast Tibetan Plateau facilitated the Cyperaceae taxa expansion and supported the plant richness increase during this period.

During the late Holocene period (5 cal ka BP to present), the study region was characterized by Poaceae-forbs meadow steppe, with high plant richness. In the pollen analysis from Lake Kuhai, both total pollen concentration and the A/Cy ratio decline from 6.3 to 2.2 cal ka BP, A/Cy ratio range between 1 and 3, which suggests alpine steppe with desert elements (Wischnewski et al., 2011). However, pollen results from Lake Koucha have a low A/Cy ratio (less than 1) that is associated with an alpine meadow environment. The different vegetation types could be attributed to regional differences or to human activity. Nevertheless, sufficient moisture is still a prerequisite to support high plant richness in our study region. Synthesizing the results of water level, oxygen isotopes, and the A/Cy ratio on the northeast Tibetan Plateau suggests a relatively humid environment during the late Holocene (Wu et al., 2023) (Fig. 8c), which is supported by the finding that high plant richness also occurred then.

4.2. Prehistorical plant composition in response to land use

The RDA suggests both moisture availability and human activity act as drivers of plant composition, with human activity explaining slightly

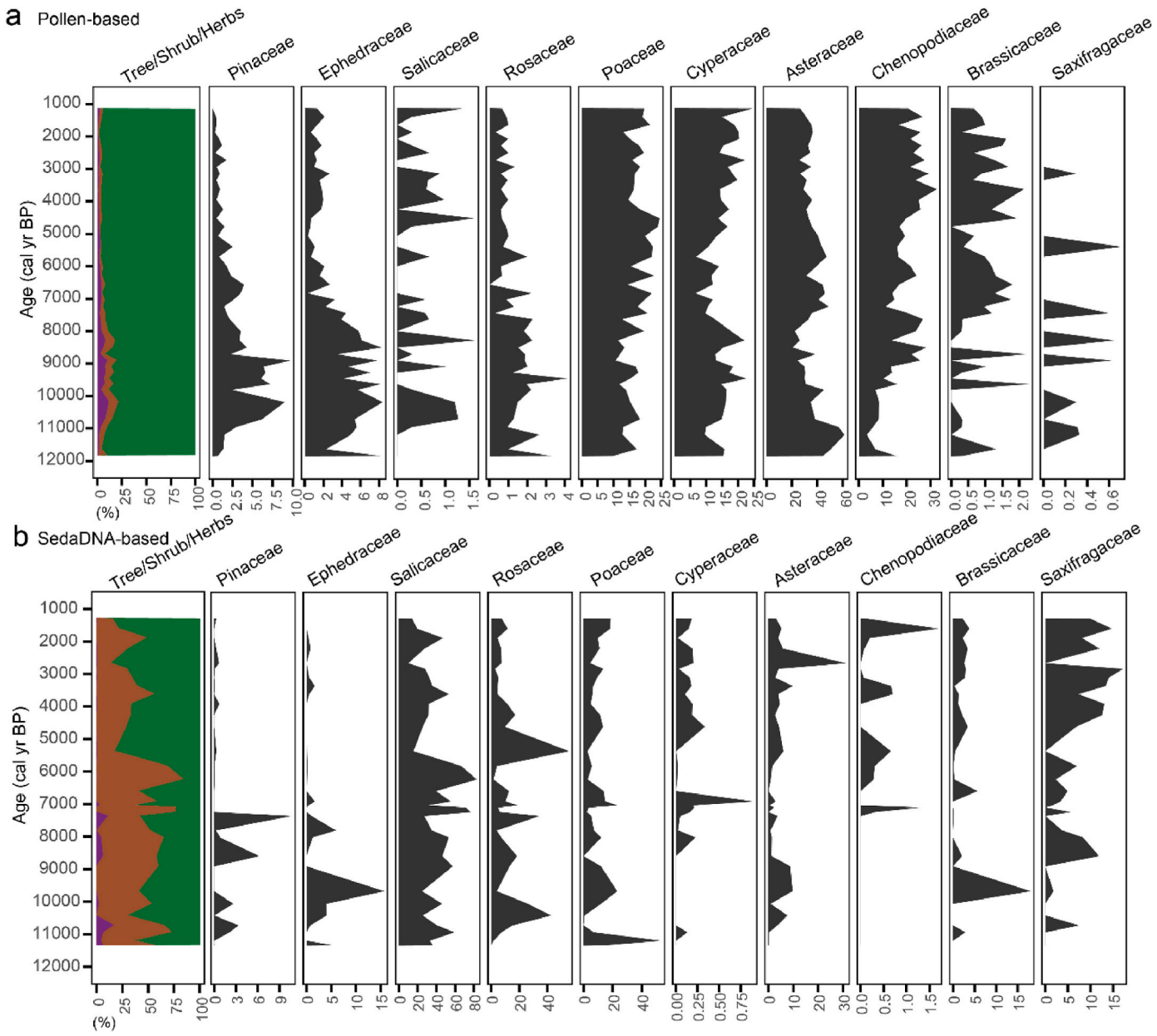

Fig. 8. Comparison of reconstructed vegetation composition based on pollen (a) and sedaDNA g/h metabarcoding (b) from Lake Donggi Cona.

more. Although most of the archaeological sites are below the elevation of Lake Donggi Cona, human activities were not confined to these locations. They may have moved to higher elevations for short-term or seasonal activities such as gathering, hunting, and grazing. Using the number of archaeological sites may overrepresent the actual human activity around the lake. Nevertheless, it can be employed to illustrate the intensity changes of human activity. Around 5 cal ka BP, despite consistently high moisture levels similar to the previous period, plant composition shifts markedly, along with an increase in human activity. Given the absence of arboreal plant taxa since the early Holocene, there was no deforestation, an activity typically associated with human disturbance of natural landscapes. By integrating sedimentary ancient DNA findings with the archaeological record of the northeast Tibetan Plateau, and the abundance of poisonous plants as an indicator to evaluate the rangeland quality, we identified two distinct stages of plant composition response to human land use: negligible influence, and notable decline in pastoral quality.

Before 4 cal ka BP (Paleolithic and Neolithic ages), minimal influence on plant composition from hunter-gatherer livelihoods is found, with relatively high pastoral quality (Fig. 10). Prior to 5 cal ka BP, the taxa comprising the abundant Poaceae, as determined by g/h metabarcoding (Fig. 3), include forage species identified by ITS1 Poaceae analysis (Fig. 6). Among these, *Puccinellia tenuiflora*, with its high protein content in stems and leaves, serves as forage and is preferred by livestock. *Stipa*, *Poa*, *Festuca*, and *Leymus* could also serve as forage, supporting the prerequisites for grazing activities (Editorial Committee of Flora of China, 1978). While Cyperaceae is less abundant during this period, the herbivore-indicator taxon, *Kobresia pygmaea,* was detected by the ITS1 Cyperaceae analysis at low abundance (Fig. 10a) (Miehe et al., 2014). Another herbivore-indicator taxon, *Potentilla anserina*, was detected by the g/h metabarcoding, also at relatively low abundance (Fig. 10e) (Wang et al., 2017). Although the genome variation study of wild and domestic yaks dates their domestication to 7.3 ka BP (Qiu et al., 2015), the zooarchaeological and ancient DNA evidence both suggest a later domestication period (Chen et al., 2023; Ren et al., 2022). The faunal remains suggest that domesticated animals were mainly omnivores

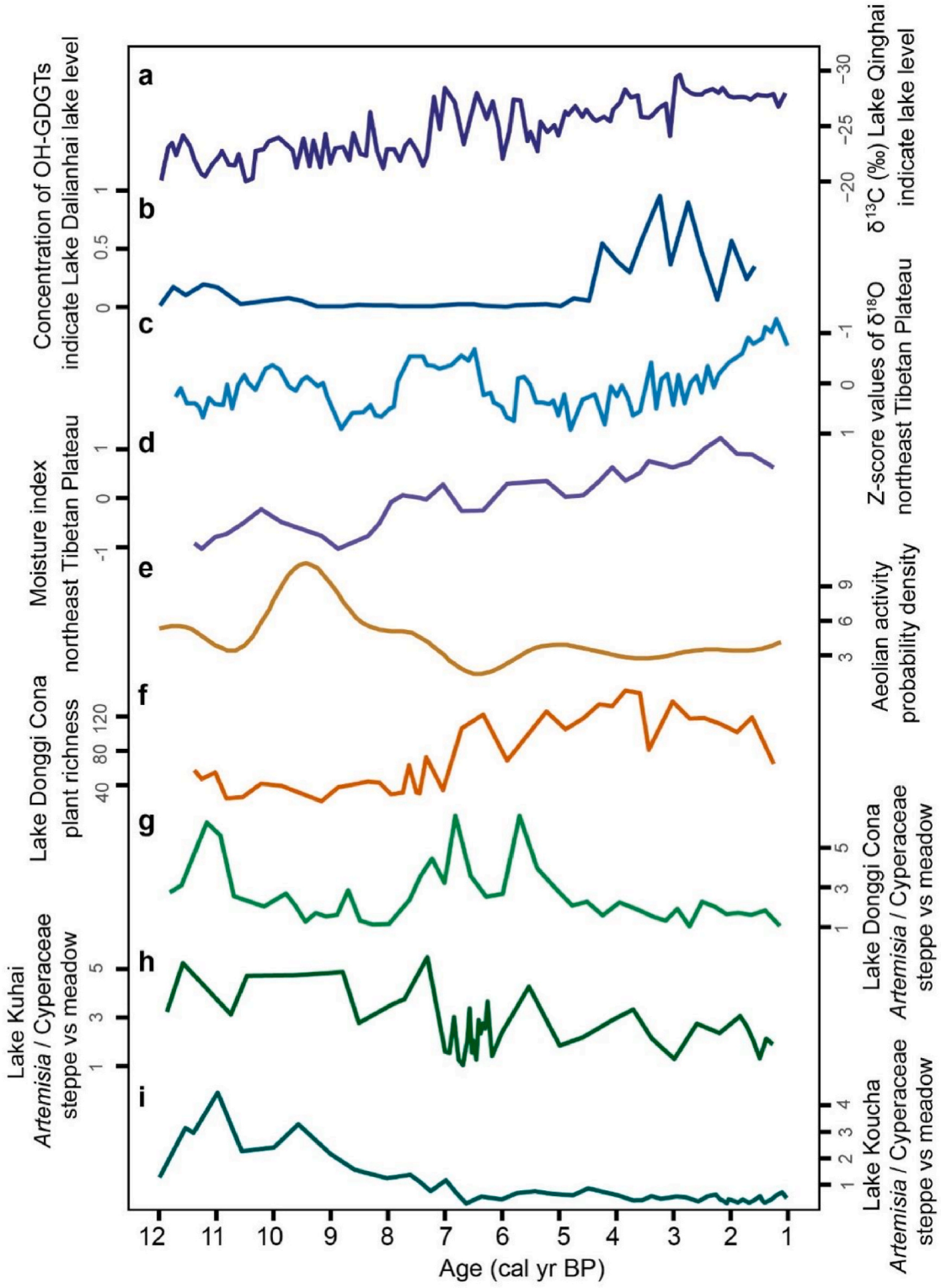

Fig. 9. Holocene paleoclimate and paleovegetation changes on the northeast Tibetan Plateau (NETP). a: Water-level change of Lake Qinghai reconstructed from $\delta^{13}C$ (higher value corresponds to lower lake levels) (Liu et al., 2013); b: Concentration of OH-GDGTs of Lake Dalianhai (higher value corresponds to higher lake levels) (Wu et al., 2020); c: Z-score of the $\delta^{18}O$ records from the northeast Tibetan Plateau (NETP) (Wu et al., 2022); d: Integrated Holocene effective moisture index for the northeast Tibetan Plateau (integration of seven records from: i) Lake Qinghai OH-GDGTs concentration, ii) authigenic carbonate $\delta^{18}O$ from Lake Hurleg, iii) Lake Genggahai $\delta^{18}O$, iv) Lake Dalianhai $\delta^{18}O$, v) Lake Donggi Cona $\delta^{18}O$, vi) *Artemisia*/Chenopodiaceae (A/C) pollen ratio from Lake Genggahai, vii) magnetic susceptibility record from the BSY19A loess-paleosol sequence) (Wu et al., 2023); e: Probability density function plot for OSL ages of aeolian sand sections from NETP (Chen et al., 2016); f: Total plant richness change based on the sedaDNA g/h primer result of Lake Donggi Cona; g: *Artemisia*/Cyperaceae (A/Cy) of Lake Donggi Cona (Wang et al., 2014); h: A/Cy of Lake Kuhai (Wischnewski et al., 2011); i: A/Cy of Lake Koucha(Herzschuh et al., 2009).

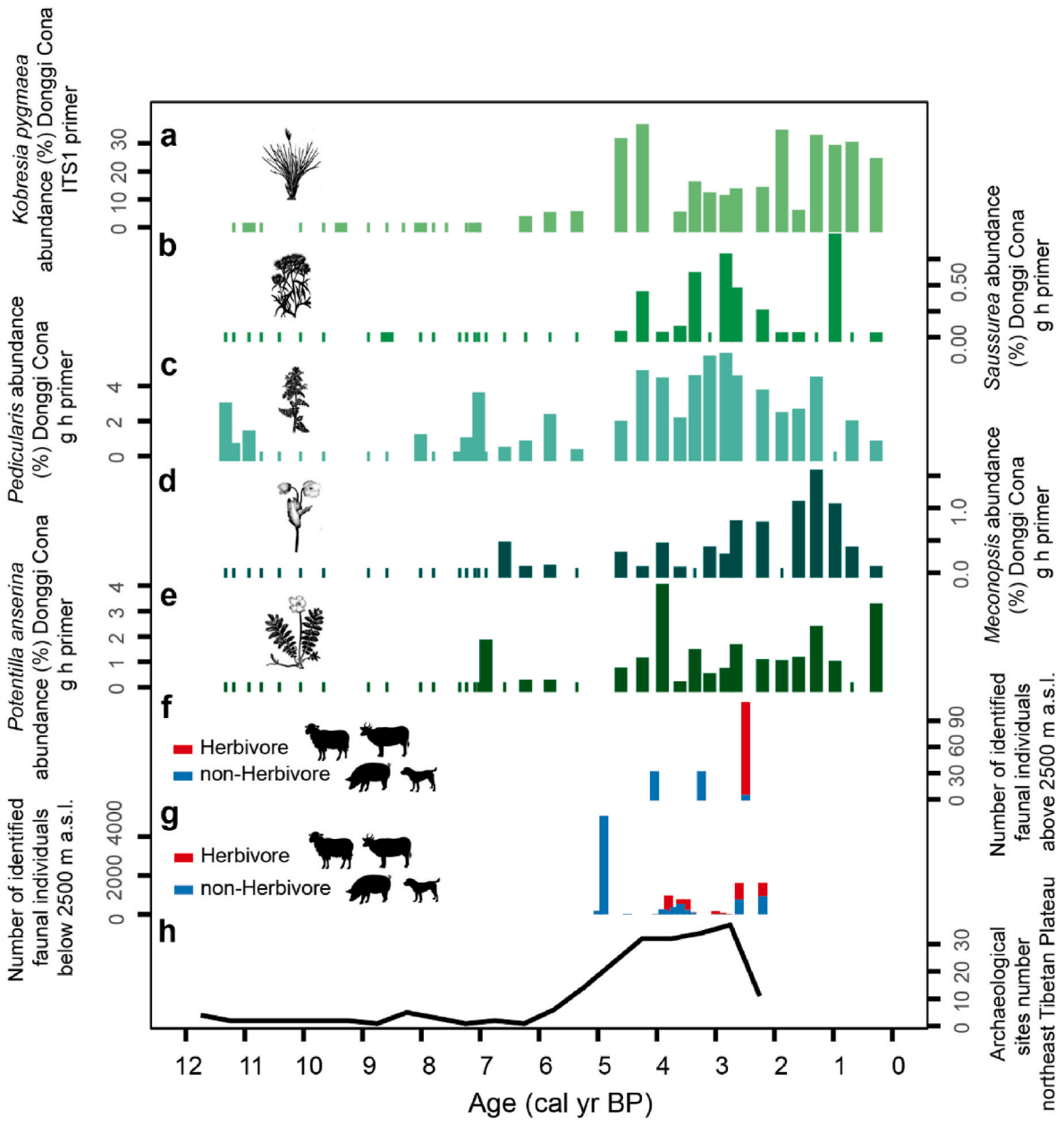

Fig. 10. Holocene rangeland taxa signals in response to herbivore activities on the northeast Tibetan Plateau (NETP). a: *Kobresia pygmaea* abundance (indicating herbivore activity (Miehe et al., 2014)) based on the ITS1 Cyperaceae metabarcoding result of Lake Donggi Cona; b: *Saussurea* abundance (indicating herbivore activity (Schlütz and Lehmkuhl, 2009)), c: *Pedicularis* spp. (poisonous plants (Qin et al., 2022)) abundance, d: *Meconopsis* spp. (poisonous plants (Ma et al., 2015)), and e: *Potentilla anserina* (indicator species for livestock hotspots (Wang et al., 2017)) abundance, all based on the gh metabarcoding result of Lake Donggi Cona; f: Number of domesticated faunal individual remains above 2500 m a.s.l. and g: below 2500 m a.s.l. on the NETP (Ren and Ren, 2024); h: Number of prehistoric archaeological sites on the NETP and contiguous regions (Cao and Dong, 2020).

(dogs and pigs) in both high and low-elevation regions (Ren and Ren, 2024) (Fig. 10g). Additionally, dated archaeological findings are relatively few, and are primarily characterized by stone tools used for hunting game (Cao and Dong, 2020). Between 5 and 4 cal ka BP, taxa associated with pastoralism such as *Kobresia pygmaea* show an increase in abundance (Fig. 10a). In addition, the number of archaeological sites increase during this period,. However, the faunal remains show the domesticated animals are non-herbivores (Fig. 10g) (Brunson et al., 2020; Ren and Ren, 2024) Therefore, whether the slight decline in pasture quality is due to human herding activities remains to be investigated. Overall, prior to 4 cal ka BP, the influence of human-induced grazing activities was limited, resulting in the low abundance of taxa associated with rangeland degradation and suggesting relatively high pastoral quality.

After 4 cal ka BP (the Bronze Age), intensified nomadic activities led to a severe decline in pastoral quality. The continuous presence of *Kobresia pygmaea*, Saussurea spp., and *Potentilla anserina* at relatively high abundances suggests intensified herbivore activity (Fig. 10a, b, 10e), supported by the persistent occurrence of Poaceae. Meanwhile, increasing abundances of *Pedicularis* spp. and *Meconopsis* spp. suggest further rangeland quality degradation (Fig. 10c and d). During this period, cold-tolerant barley and sheep were introduced and people settled in higher-elevation areas permanently (Cao and Dong, 2020; Chen et al., 2015), and an agro-pastoral economy developed on the northeast Tibetan Plateau. Herbivores, in particular, dominated the domesticated animals in the high-elevation areas as inferred from the

zooarchaeological evidence (Ren and Ren, 2024) (Fig. 10f). However, in low-elevation areas, the proportion of herbivores to non-herbivores is similar (Fig. 10g). Thus, human migration towards higher elevations exacerbated herbivore grazing activities, resulting in severe rangeland quality decline.

4.3. Plant richness changes with climate and human activity

Our results show that the highest plant richness was during the late Holocene, associated with relatively high moisture availability and intensified human activity. In contrast, the plant richness of Lake Naleng, located on the southeastern margin of the Tibetan Plateau, is highest between 14 and 10 cal ka BP (Liu et al., 2021). This discrepancy primarily arises from different restriction factors between these two study regions. Alpine habitat is the limiting factor around Lake Naleng, with livestock grazing only weakly promoting plant richness in this cold climate-impacted habitat. Conversely, in the semi-arid Lake Donggi Cona region, moisture availability and human activity more easily influence plant richness.

The generalized additive models (GAMs) show statistically significant non-linear patterns of plant richness and both effective moisture ($p < 0.05$, $R^2(adj) = 0.384$) and human activity ($p < 0.05$, $R^2(adj) = 0.661$) with human activity explaining more (Supplementary Fig. 2a). As effective moisture increases, plant richness trends upwards. Especially around 7.4 cal ka BP, when human activity is negligible, plant richness increases pronouncedly with high moisture availability. According to the "water-energy dynamic hypothesis" (O' Brien, 1998), water and energy are the two main factors to explain the globally extensive plant diversity gradient. In our study region, which is dominated by a semi-arid environment (Knapp et al., 2002; Li, 2018), higher moisture availability supports more diverse plant taxa colonization (Deng et al., 2016), which is in line with the "water-energy dynamic hypothesis".

With human density increasing, plant richness increases as well, and peaks during the prehistoric human activity intensification period (Supplementary Fig. 2b). In central Europe, human-induced deforestation had a much greater impact on plant diversity than climate change (Giesecke et al., 2019), becoming the dominant driver of plant richness in the late Holocene. While pollen analysis suggests plant richness declines due to human activity in eastern China (Cao et al., 2022), the dominant human effects are attributed to deforestation in eastern China but to pastoralism in our study region. These factors may drive richness change in different directions. Contrary to previous studies suggesting that intensified grazing activity can diminish plant diversity (Liu et al., 2023), our study proposes an alternative perspective. It is plausible that herbivory suppresses dominant taxa, reducing plant competition (Pulungan et al., 2019), which, when coupled with the enhanced nutrient and light availability for grazing-tolerant species (Li et al., 2013; Lu et al., 2017), could increase and sustain grassland richness. This may be particularly relevant in our study region, which is characterized by high elevation and a harsh environment. Human activity may also elevate spatial heterogeneity, and enhance niche breadth and overlap, facilitating species coexistence (McGranahan et al., 2012). Furthermore, the intermediate disturbance hypothesis suggests that moderate disturbance levels promote community succession, maintaining community structure and species diversity (Kiełtyk and Mirek, 2015), which could also explain the grazing-related richness increase.

Within the different plant families, all demonstrate relatively high richness during the middle-late Holocene period (Supplementary Fig. 3). Our GAMs indicate that for most plant families, richness increases linearly with moisture, except for Poaceae. Poaceae richness is relatively stable at low and moderate moisture availability, although the richness does increase when moisture availability is high. Prehistorical human activity corresponds with increased richness for all plant families (Supplementary Fig. 4). With regard to future grassland conservation, the diversity of Poaceae may be more resistant to climate change.

5. Conclusions

This study used sedimentary ancient DNA employing two methods – g/h metabarcoding and ITS1 metabarcoding for Poaceae and Cyperaceae – to evaluate the impact of climate change and human activity on rangeland characteristics. We find that drought-adapted taxa disappear and plant richness increases with rising effective moisture. Human activity uniquely explains more of the plant composition and richness change although there is a large amount of shared covariance. During the late Holocene period, pastoralism led to an increase in poisonous plant abundance, decreasing pasture quality yet enhancing rangeland richness. The ITS1 metabarcoding method particularly enhances our ability to detect pastoralism-related taxa, improving the evaluation of grazing activity impacts. To forecast rangeland development and conservation, human activity needs to be given primary consideration.

Authorship contribution statement

Ying Liu: Conceptualization, Methodology, Software, Formal analysis, Investigation, Data curation, Writing – original draft, Visualization. **Kathleen R. Stoof-Leichsenring:** Methodology, Writing – review & editing. **Bernhard Diekmann:** Resources, Writing – review & editing. **Ulrike Herzschuh:** Conceptualization, Resources, Writing – review & editing, Supervision.

Declaration of competing interest

The authors declare that they have no known competing financial interests or personal relationships that could have appeared to influence the work reported in this paper.

Data availability

DNA sequence data for this study have been deposited in the European Nucleotide Archive (ENA) at EMBL-EBI under accession number PRJEB77355 (https://www.ebi.ac.uk/ena/browser/view/PRJEB77355). The tag files required to identify the samples are provided in Supplementary files.

Acknowledgments

We would like to express our gratitude to the editor Dr. Patrick Rioual, and the two anonymous reviewers for their valuable feedback, which has strengthened this paper. We also thank Cathy Jenks at the University of Bergen for proofreading this manuscript. This research has been supported by the European Research Council (ERC Glacial Legacy 772852 to Ulrike Herzschuh), and China Scholarship Council (grant 202106620011 to Ying Liu).

Appendix A. Supplementary data

Supplementary data to this article can be found online at https://doi.org/10.1016/j.quascirev.2024.108850.

References

Ait Baamrane, M.A., Shehzad, W., Ouhammou, A., Abbad, A., Naimi, M., Coissac, E., Taberlet, P., Znari, M., 2012. Assessment of the food habits of the Moroccan Dorcas Gazelle in M'Sabih Talaa, west Central Morocco, using the trnL approach. PLoS One 7, e35643. https://doi.org/10.1371/journal.pone.0035643.

Bardgett, R.D., Bullock, J.M., Lavorel, S., Manning, P., Schaffner, U., Ostle, N., Chomel, M., Durigan, G., L. Fry, E., Johnson, D., Lavallee, J.M., Le Provost, G., Luo, S., Png, K., Sankaran, M., Hou, X., Zhou, H., Ma, L., Ren, W., Li, X., Ding, Y., Li, Y., Shi, H., 2021. Combatting global grassland degradation. Nat. Rev. Earth Environ. 2, 720–735. https://doi.org/10.1038/s43017-021-00207-2.

Bellemain, E., Carlsen, T., Brochmann, C., Coissac, E., Taberlet, P., Kauserud, H., 2010. ITS as an environmental DNA barcode for fungi: an *in silico* approach reveals potential PCR biases. BMC Microbiol. 10, 189. https://doi.org/10.1186/1471-2180-10-189.

Blaauw, M., Christen, J.A., 2011. Flexible paleoclimate age-depth models using an autoregressive gamma process. Bayesian Analysis 6, 457–474. https://doi.org/10.1214/11-BA618.

Boyer, F., Mercier, C., Bonin, A., Le Bras, Y., Taberlet, P., Coissac, E., 2016. OBITOOLS : a UNIX-inspired software package for DNA metabarcoding. Molecular Ecology Resources 16, 176–182. https://doi.org/10.1111/1755-0998.12428.

Brunson, K., Lele, R., Xin, Z., Xiaoling, D., Hui, W., Jing, Z., Flad, R., 2020. Zooarchaeology, ancient mtDNA, and radiocarbon dating provide new evidence for the emergence of domestic cattle and caprines in the Tao River Valley of Gansu Province, northwest China. J. Archaeol. Sci.: Report 31, 102262. https://doi.org/10.1016/j.jasrep.2020.102262.

Cao, H., Dong, G., 2020. Social development and living environment changes in the Northeast Tibetan Plateau and contiguous regions during the late prehistoric period. Regional Sustainability 1, 59–67. https://doi.org/10.1016/j.regsus.2020.09.001.

Cao, X., Tian, F., Herzschuh, U., Ni, J., Xu, Q., Li, W., Zhang, Y., Luo, M., Chen, F., 2022. Human activities have reduced plant diversity in eastern China over the last two millennia. Global Change Biol. 28, 4962–4976. https://doi.org/10.1111/gcb.16274.

Chao, A., Gotelli, N.J., Hsieh, T.C., Sander, E.L., Ma, K.H., Colwell, R.K., Ellison, A.M., 2014. Rarefaction and extrapolation with Hill numbers: a framework for sampling and estimation in species diversity studies. Ecol. Monogr. 84 (1), 45–67. https://doi.org/10.1890/13-0133.

Chen, F.H., Dong, G.H., Zhang, D.J., Liu, X.Y., Jia, X., An, C.B., Ma, M.M., Xie, Y.W., Barton, L., Ren, X.Y., Zhao, Z.J., Wu, X.H., Jones, M.K., 2015. Agriculture facilitated permanent human occupation of the Tibetan Plateau after 3600 B.P. Science 347, 248–250. https://doi.org/10.1126/science.1259172.

Chen, F., Wu, D., Chen, J., Zhou, A., Yu, J., Shen, J., Wang, S., Huang, X., 2016. Holocene moisture and East Asian summer monsoon evolution in the northeastern Tibetan Plateau recorded by Lake Qinghai and its environs: a review of conflicting proxies. Quat. Sci. Rev. 154, 111–129. https://doi.org/10.1016/j.quascirev.2016.10.021.

Chen, F., Welker, F., Shen, C.-C., Bailey, S.E., Bergmann, I., Davis, S., Xia, H., Wang, H., Fischer, R., Freidline, S.E., Yu, T.-L., Skinner, M.M., Stelzer, S., Dong, G., Fu, Q., Dong, G., Wang, J., Zhang, D., Hublin, J.-J., 2019. A late middle Pleistocene Denisovan mandible from the Tibetan plateau. Nature 569, 409–412. https://doi.org/10.1038/s41586-019-1139-x.

Chen, N., Zhang, Z., Hou, J., Chen, J., Gao, X., Tang, L., Wangdue, S., Zhang, X., Sinding, M.-H.S., Liu, Xuexue, Han, J., Lü, H., Lei, C., Marshall, F., Liu, Xinyi, 2023. Evidence for early domestic yak, taurine cattle, and their hybrids on the Tibetan Plateau. Sci. Adv. 9, eadi6857 https://doi.org/10.1126/sciadv.adi6857.

Cheng, B., Chen, F., Zhang, J., 2013. Palaeovegetational and palaeoenvironmental changes since the last deglacial in Gonghe Basin, northeast Tibetan Plateau. J. Geogr. Sci. 23, 136–146. https://doi.org/10.1007/s11442-013-0999-5.

Deng, L., Wang, K., Li, J., Zhao, G., Shangguan, Z., 2016. Effect of soil moisture and atmospheric humidity on both plant productivity and diversity of native grasslands across the Loess Plateau, China. Ecol. Eng. 94, 525–531. https://doi.org/10.1016/j.ecoleng.2016.06.048.

Dietze, E., Wünnemann, B., Diekmann, B., Aichner, B., Hartmann, K., Herzschuh, U., IJmker, J., Jin, H., Kopsch, C., Lehmkuhl, F., Li, S., Mischke, S., Niessen, F., Opitz, S., Stauch, G., Yang, S., 2010. Basin morphology and seismic stratigraphy of Lake Donggi Cona, north-eastern Tibetan plateau, China. Quat. Int. 218, 131–142. https://doi.org/10.1016/j.quaint.2009.11.035.

Dietze, E., Wünnemann, B., Hartmann, K., Diekmann, B., Jin, H., Stauch, G., Yang, S., Lehmkuhl, F., 2013. Early to mid-Holocene lake high-stand sediments at Lake Donggi Cona, northeastern Tibetan Plateau, China. Quat. Res. 79, 325–336. https://doi.org/10.1016/j.yqres.2012.12.008.

Dong, G., Yang, Y., Liu, X., Li, H., Cui, Y., Wang, H., Chen, G., Dodson, J., Chen, F., 2018. Prehistoric trans-continental cultural exchange in the Hexi Corridor, northwest China. Holocene 28, 621–628. https://doi.org/10.1177/0959683617735585.

Editorial Committee of Flora of China, 1978. Flora of China. Science Press.

Chen, F., Zhang, J., Liu, J., Cao, X., Hou, J., Zhu, L., Xu, X., Liu, X., Wang, M., Wu, D., Huang, L., Zeng, T., Zhang, S., Huang, W., Zhang, X., Yang, K., 2020. Climate change, vegetation history, and landscape responses on the Tibetan Plateau during the Holocene: a comprehensive review. Quat. Sci. Rev. 243, 106444 https://doi.org/10.1016/j.quascirev.2020.106444.

Ficetola, G., Coissac, E., Zundel, S., Riaz, T., Shehzad, W., Bessière, J., Taberlet, P., Pompanon, F., 2010. An *In silico* approach for the evaluation of DNA barcodes. BMC Genom. 11, 434. https://doi.org/10.1186/1471-2164-11-434.

Garcés-Pastor, S., Coissac, E., Lavergne, S., Schwörer, C., Theurillat, J.-P., Heintzman, P. D., Wangensteen, O.S., Tinner, W., Rey, F., Heer, M., Rutzer, A., Walsh, K., Lammers, Y., Brown, A.G., Goslar, T., Rijal, D.P., Karger, D.N., Pellissier, L., The, PhyloAlps Consortium, Heiri, O., Alsos, I.G., 2022. High resolution ancient sedimentary DNA shows that alpine plant diversity is associated with human land use and climate change. Nat. Commun. 13, 6559. https://doi.org/10.1038/s41467-022-34010-4.

Giesecke, T., Wolters, S., Van Leeuwen, J.F.N., Van Der Knaap, P.W.O., Leydet, M., Brewer, S., 2019. Postglacial change of the floristic diversity gradient in Europe. Nat. Commun. 10, 5422. https://doi.org/10.1038/s41467-019-13233-y.

Goring, S., Lacourse, T., Pellatt, M.G., Mathewes, R.W., 2013. Pollen assemblage richness does not reflect regional plant species richness: a cautionary tale. J. Ecol. 101, 1137–1145. https://doi.org/10.1111/1365-2745.12135.

Gosling, W.D., Julier, A.C.M., Adu-Bredu, S., Djagbletey, G.D., Fraser, W.T., Jardine, P.E., Lomax, B.H., Malhi, Y., Manu, E.A., Mayle, F.E., Moore, S., 2018. Pollen-vegetation richness and diversity relationships in the tropics. Veg. Hist. Archaeobotany 27, 411–418. https://doi.org/10.1007/s00334-017-0642-y.

Grimm, E.C., 1987. CONISS: a FORTRAN 77 program for stratigraphically constrained cluster analysis by the method of incremental sum of squares. Comput. Geosci. 13, 13–35. https://doi.org/10.1016/0098-3004(87)90022-7.

Heaton, T.J., Köhler, P., Butzin, M., Bard, E., Reimer, R.W., Austin, W.E.N., Bronk Ramsey, C., Grootes, P.M., Hughen, K.A., Kromer, B., Reimer, P.J., Adkins, J., Burke, A., Cook, M.S., Olsen, J., Skinner, L.C., 2020. Marine20—the marine radiocarbon age calibration Curve (0–55,000 cal BP). Radiocarbon 62, 779–820. https://doi.org/10.1017/RDC.2020.68.

Herzschuh, U., 2006. Palaeo-moisture evolution in monsoonal Central Asia during the last 50,000 years. Quat. Sci. Rev. 25, 163–178. https://doi.org/10.1016/j.quascirev.2005.02.006.

Herzschuh, U., Kramer, A., Mischke, S., Zhang, C., 2009. Quantitative climate and vegetation trends since the late glacial on the northeastern Tibetan Plateau deduced from Koucha Lake pollen spectra. Quat. Res. 71, 162–171. https://doi.org/10.1016/j.yqres.2008.09.003.

Herzschuh, U., Ni, J., Birks, H.J.B., Böhner, J., 2011. Driving forces of mid-Holocene vegetation shifts on the upper Tibetan Plateau, with emphasis on changes in atmospheric CO_2 concentrations. Quat. Sci. Rev. 30, 1907–1917. https://doi.org/10.1016/j.quascirev.2011.03.007.

Hill, M.O., Gauch, H.G., 1980. Detrended correspondence analysis: an improved ordination technique. Vegetatio 42, 47–58. https://doi.org/10.1007/BF00048870.

Jia, W., Anslan, S., Chen, F., Cao, X., Dong, H., Dulias, K., Gu, Z., Heinecke, L., Jiang, H., Kruse, S., Kang, W., Li, K., Liu, S., Liu, X., Liu, Y., Ni, J., Schwalb, A., Stoof-Leichsenring, K.R., Shen, W., Tian, F., Wang, J., Wang, Yongbo, Wang, Yucheng, Xu, H., Yang, X., Zhang, D., Herzschuh, U., 2022. Sedimentary ancient DNA reveals past ecosystem and biodiversity changes on the Tibetan Plateau: overview and prospects. Quat. Sci. Rev. 293, 107703 https://doi.org/10.1016/j.quascirev.2022.107703.

Kiełtyk, P., Mirek, Z., 2015. Importance of molehill disturbances for invasion by *Bunias orientalis* in meadows and pastures. Acta Oecol. 64, 29–34. https://doi.org/10.1016/j.actao.2015.02.007.

Knapp, A.K., Fay, P.A., Blair, J.M., Collins, S.L., Smith, M.D., Carlisle, J.D., Harper, C.W., Danner, B.T., Lett, M.S., McCarron, J.K., 2002. Rainfall variability, carbon cycling, and plant species diversity in a Mesic grassland. Science 298, 2202–2205. https://doi.org/10.1126/science.1076347.

Kramer, A., Herzschuh, U., Mischke, S., Zhang, C., 2010. Holocene treeline shifts and monsoon variability in the Hengduan Mountains (southeastern Tibetan Plateau), implications from palynological investigations. Palaeogeogr. Palaeoclimatol. Palaeoecol. 286, 23–41. https://doi.org/10.1016/j.palaeo.2009.12.001.

Li, D., 2018. The plant functional traits of arid and Semiarid grassland plants under warming and precipitation change. In: Ratnadewi, D., Hamim (Eds.), Plant Growth and Regulation - Alterations to Sustain Unfavorable Conditions. IntechOpen. https://doi.org/10.5772/intechopen.79744.

Li, W., Tian, F.P., Ren, Z.W., Huang, H.Z., Zhang, Z.N., 2013. Effects of grazing and fertilization on the relationship between species abundance and functional traits in an alpine meadow community on the Tibetan Plateau. Nord. J. Bot. 31, 247–255. https://doi.org/10.1111/j.1756-1051.2012.01511.x.

Li, Y., Qiang, M., Huang, X., Zhao, Y., Leppänen, J.J., Weckström, J., Väliranta, M., 2021. Lateglacial and Holocene climate change in the NE Tibetan Plateau: reconciling divergent proxies of Asian summer monsoon variability. Catena 199, 105089. https://doi.org/10.1016/j.catena.2020.105089.

Liu, W., Li, X., An, Z., Xu, L., Zhang, Q., 2013. Total organic carbon isotopes: a novel proxy of lake level from Lake Qinghai in the Qinghai–Tibet Plateau, China. Chem. Geol. 347, 153–160. https://doi.org/10.1016/j.chemgeo.2013.04.009.

Liu, S., Kruse, S., Scherler, D., Ree, R.H., Zimmermann, H.H., Stoof-Leichsenring, K.R., Epp, L.S., Mischke, S., Herzschuh, U., 2021. Sedimentary ancient DNA reveals a threat of warming-induced alpine habitat loss to Tibetan Plateau plant diversity. Nat. Commun. 12, 2995. https://doi.org/10.1038/s41467-021-22986-4.

Liu, M., Yin, F., Xiao, Y., Yang, C., 2023. Grazing alters the relationship between alpine meadow biodiversity and ecosystem multifunctionality. Sci. Total Environ. 898, 165445 https://doi.org/10.1016/j.scitotenv.2023.165445.

Liu, S., Stoof-Leichsenring, K.R., Harms, L., Schulte, L., Mischke, S., Kruse, S., Zhang, C. J., Herzschuh, U., 2024. Tibetan terrestrial and aquatic ecosystems collapsed with cryosphere loss inferred from sedimentary ancient metagenomics. Sci. Adv. 10, eadn8490 https://doi.org/10.1126/sciadv.adn8490.

Lu, X., Kelsey, K.C., Yan, Y., Sun, J., Wang, X., Cheng, G., Neff, J.C., 2017. Effects of grazing on ecosystem structure and function of alpine grasslands in Qinghai–Tibetan Plateau: a synthesis. Ecosphere 8, e01656. https://doi.org/10.1002/ecs2.1656.

Ma, L., Gu, R., Tang, L., Chen, Z.-E., Di, R., Long, C., 2015. Important poisonous plants in Tibetan ethnomedicine. Toxins 7, 138–155. https://doi.org/10.3390/toxins7010138.

McGranahan, D.A., Engle, D.M., Fuhlendorf, S.D., Winter, S.J., Miller, J.R., Debinski, D. M., 2012. Spatial heterogeneity across five rangelands managed with pyric-herbivory. J. Appl. Ecol. 49, 903–910. https://doi.org/10.1111/j.1365-2664.2012.02168.x.

Miehe, G., Miehe, S., Böhner, J., Kaiser, K., Hensen, I., Madsen, D., Liu, J., Opgenoorth, L., 2014. How old is the human footprint in the world's largest alpine ecosystem? A review of multiproxy records from the Tibetan Plateau from the ecologists' viewpoint. Quat. Sci. Rev. 86, 190–209. https://doi.org/10.1016/j.quascirev.2013.12.004.

Mischke, S., Aichner, B., Diekmann, B., Herzschuh, U., Plessen, B., Wünnemann, B., Zhang, C., 2010a. Ostracods and stable isotopes of a late glacial and Holocene lake record from the NE Tibetan Plateau. Chem. Geol. 276, 95–103. https://doi.org/10.1016/j.chemgeo.2010.06.003.

Mischke, S., Bößneck, U., Diekmann, B., Herzschuh, U., Jin, H., Kramer, A., Wünnemann, B., Zhang, C., 2010b. Quantitative relationship between water-depth and sub-fossil ostracod assemblages in Lake Donggi Cona, Qinghai Province, China. J. Paleolimnol. 43, 589–608. https://doi.org/10.1007/s10933-009-9355-2.

Oksanen, J., Blanchet, F.G., Kindt, R., Legendre, P., Minchin, P.R., O'Hara, R.B., Simpson, G.L., Solymos, P., Stevens, M.H.H., Wagner, H., 2022. Vegan: community ecology package. R package version 2, 6-4.

Opitz, S., Wünnemann, B., Aichner, B., Dietze, E., Hartmann, K., Herzschuh, U., IJmker, J., Lehmkuhl, F., Li, S., Mischke, S., Plotzki, A., Stauch, G., Diekmann, B., 2012. Late glacial and Holocene development of Lake Donggi Cona, north-eastern Tibetan plateau, inferred from sedimentological analysis. Palaeogeogr. Palaeoclimatol. Palaeoecol. 337–338, 159–176. https://doi.org/10.1016/j.palaeo.2012.04.013.

Opitz, S., Ramisch, A., IJmker, J., Lehmkuhl, F., Mischke, S., Stauch, G., Wünnemann, B., Zhang, Y., Diekmann, B., 2016. Spatio-temporal pattern of detrital clay-mineral supply to a lake system on the north-eastern Tibetan Plateau, and its relationship to late Quaternary paleoenvironmental changes. Catena 137, 203–218. https://doi.org/10.1016/j.catena.2015.09.003.

O' Brien, E., 1998. Water-energy dynamics, climate, and prediction of woody plant species richness: an interim general model. J. Biogeogr. 25, 379–398. https://doi.org/10.1046/j.1365-2699.1998.252166.x.

Pedersen, M.W., Ginolhac, A., Orlando, L., Olsen, J., Andersen, K., Holm, J., Funder, S., Willerslev, E., Kjær, K.H., 2013. A comparative study of ancient environmental DNA to pollen and macrofossils from lake sediments reveals taxonomic overlap and additional plant taxa. Quat. Sci. Rev. 75, 161–168. https://doi.org/10.1016/j.quascirev.2013.06.006.

Pulungan, M.A., Suzuki, S., Gavina, M.K.A., Tubay, J.M., Ito, H., Nii, M., Ichinose, G., Okabe, T., Ishida, A., Shiyomi, M., Togashi, T., Yoshimura, J., Morita, S., 2019. Grazing enhances species diversity in grassland communities. Sci. Rep. 9, 11201 https://doi.org/10.1038/s41598-019-47635-1.

Qiang, M., Jin, Y., Liu, X., Song, L., Li, H., Li, F., Chen, F., 2016. Late Pleistocene and Holocene aeolian sedimentation in Gonghe basin, northeastern Qinghai-Tibetan plateau: variability, processes, and climatic implications. Quat. Sci. Rev. 132, 57–73. https://doi.org/10.1016/j.quascirev.2015.11.010.

Qin, R., Wei, J., Ma, L., Zhang, Z., She, Y., Su, H., Chang, T., Xie, B., Li, H., Wang, W., Shi, G., Zhou, H., 2022. Effects of Pedicularis kansuensis expansion on plant community characteristics and soil nutrients in an alpine grassland. Plants 11, 1673. https://doi.org/10.3390/plants11131673.

Qiu, Q., Wang, L., Wang, K., Yang, Y., Ma, T., Wang, Z., Zhang, X., Ni, Z., Hou, F., Long, R., Abbott, R., Lenstra, J., Liu, J., 2015. Yak whole-genome resequencing reveals domestication signatures and prehistoric population expansions. Nat. Commun. 6, 10283 https://doi.org/10.1038/ncomms10283.

Reimer, P.J., Austin, W.E.N., Bard, E., Bayliss, A., Blackwell, P.G., Bronk Ramsey, C., Butzin, M., Cheng, H., Edwards, R.L., Friedrich, M., Grootes, P.M., Guilderson, T.P., Hajdas, I., Heaton, T.J., Hogg, A.G., Hughen, K.A., Kromer, B., Manning, S.W., Muscheler, R., Palmer, J.G., Pearson, C., Van Der Plicht, J., Reimer, R.W., Richards, D.A., Scott, E.M., Southon, J.R., Turney, C.S.M., Wacker, L., Adolphi, F., Büntgen, U., Capano, M., Fahrni, S.M., Fogtmann-Schulz, A., Friedrich, R., Köhler, P., Kudsk, S., Miyake, F., Olsen, J., Reinig, F., Sakamoto, M., Sookdeo, A., Talamo, S., 2020. The IntCal20 northern hemisphere radiocarbon age calibration Curve (0–55 cal kBP). Radiocarbon 62, 725–757. https://doi.org/10.1017/RDC.2020.41.

Ren, K., Ren, L., 2024. Faunal remains data from Paleolithic-early Iron age archaeological sites in the Qinghai-Tibet Plateau in China. Sci. Data 11, 9. https://doi.org/10.1038/s41597-023-02858-w.

Ren, L., Yang, Y., Qiu, M., Brunson, K., Chen, G., Dong, G., 2022. Direct dating of the earliest domesticated cattle and caprines in northwestern China reveals the history of pastoralism in the Gansu-Qinghai region. J. Archaeol. Sci. 144, 105627 https://doi.org/10.1016/j.jas.2022.105627.

Rijal, D.P., Heintzman, P.D., Lammers, Y., Yoccoz, N.G., Lorberau, K.E., Pitelkova, I., Goslar, T., Murguzur, F.J.A., Salonen, J.S., Helmens, K.F., Bakke, J., Edwards, M.E., Alm, T., Bråthen, K.A., Brown, A.G., Alsos, I.G., 2021. Sedimentary ancient DNA shows terrestrial plant richness continuously increased over the Holocene in northern Fennoscandia. Sci. Adv. 7, eabf9557. https://doi.org/10.1126/sciadv.abf9557.

Schlütz, F., Lehmkuhl, F., 2009. Holocene climatic change and the nomadic Anthropocene in Eastern Tibet: palynological and geomorphological results from the Nianbaoyeze Mountains. Quat. Sci. Rev. 28, 1449–1471. https://doi.org/10.1016/j.quascirev.2009.01.009.

Shen, J., Liu, X.Q., Wang, S.M., Ryo, M., 2005. Palaeoclimatic changes in the Qinghai Lake area during the last 18,000 years. Quat. Int. 136, 131–140. https://doi.org/10.1016/j.quaint.2004.11.014.

Soininen, E.M., Gauthier, G., Bilodeau, F., Berteaux, D., Gielly, L., Taberlet, P., Gussarova, G., Bellemain, E., Hassel, K., Stenøien, H.K., Epp, L., Schrøder-Nielsen, A., Brochmann, C., Yoccoz, N.G., 2015. Highly overlapping winter diet in two sympatric Lemming species revealed by DNA metabarcoding. PLoS One 10, e0115335. https://doi.org/10.1371/journal.pone.0115335.

Sønstebø, J.H., Gielly, L., Brysting, A.K., Elven, R., Edwards, M., Haile, J., Willerslev, E., Coissac, E., Rioux, D., Sannier, J., Taberlet, P., Brochmann, C., 2010. Using next-generation sequencing for molecular reconstruction of past Arctic vegetation and climate. Molecular Ecology Resources 10, 1009–1018. https://doi.org/10.1111/j.1755-0998.2010.02855.x.

Stauch, G., IJmker, J., Pötsch, S., Zhao, H., Hilgers, A., Diekmann, B., Dietze, E., Hartmann, K., Opitz, S., Wünnemann, B., Lehmkuhl, F., 2012. Aeolian sediments on the north-eastern Tibetan Plateau. Quat. Sci. Rev. 57, 71–84. https://doi.org/10.1016/j.quascirev.2012.10.001.

Taberlet, P., Coissac, E., Pompanon, F., Gielly, L., Miquel, C., Valentini, A., Vermat, T., Corthier, G., Brochmann, C., Willerslev, E., 2007. Power and limitations of the chloroplast trnL (UAA) intron for plant DNA barcoding. Nucleic Acids Res. 35, e14. https://doi.org/10.1093/nar/gkl938.

Valentini, A., Miquel, C., Nawaz, M.A., Bellemain, E., Coissac, E., Pompanon, F., Gielly, L., Cruaud, C., Nascetti, G., Wincker, P., Swenson, J.E., Taberlet, P., 2009. New perspectives in diet analysis based on DNA barcoding and parallel pyrosequencing: the trnL approach. Molecular Ecology Resources 9, 51–60. https://doi.org/10.1111/j.1755-0998.2008.02352.x.

Wang, Y., Herzschuh, U., 2011. Reassessment of Holocene vegetation change on the upper Tibetan Plateau using the pollen-based REVEALS model. Rev. Palaeobot. Palynol. 168, 31–40. https://doi.org/10.1016/j.revpalbo.2011.09.004.

Wang, Y., Herzschuh, U., Shumilovskikh, L.S., Mischke, S., Birks, H.J.B., Wischnewski, J., Böhner, J., Schlütz, F., Lehmkuhl, F., Diekmann, B., Wünnemann, B., Zhang, C., 2014. Quantitative reconstruction of precipitation changes on the NE Tibetan Plateau since the Last Glacial Maximum – extending the concept of pollen source area to pollen-based climate reconstructions from large lakes. Clim. Past 10, 21–39. https://doi.org/10.5194/cp-10-21-2014.

Wang, Y., Heberling, G., Görzen, E., Miehe, G., Seeber, E., Wesche, K., 2017. Combined effects of livestock grazing and abiotic environment on vegetation and soils of grasslands across Tibet. Appl. Veg. Sci. 20, 327–339. https://doi.org/10.1111/avsc.12312.

Wang, J., Xia, H., Yao, J., Shen, X., Cheng, T., Wang, Q., Zhang, D., 2020. Subsistence strategies of prehistoric hunter-gatherers on the Tibetan plateau during the last deglaciation. Sci. China Earth Sci. 63, 395–404. https://doi.org/10.1007/s11430-019-9519-8.

Wang, N., Liu, L., Hou, X., Zhang, Y., Wei, H., Cao, X., 2022a. Palynological evidence reveals an arid early Holocene for the northeast Tibetan Plateau. Clim. Past 18, 2381–2399. https://doi.org/10.5194/cp-18-2381-2022.

Wang, S., Jia, L., Cai, L., Wang, Y., Zhan, T., Huang, A., Fan, D., 2022b. Assessment of grassland degradation on the Tibetan plateau based on multi-source data. Rem. Sens. 14, 6011. https://doi.org/10.3390/rs14236011.

Wang, Y., Lv, W., Xue, K., Wang, S., Zhang, L., Hu, R., Zeng, H., Xu, X., Li, Y., Jiang, L., Hao, Y., Du, J., Sun, J., Dorji, T., Piao, S., Wang, C., Luo, C., Zhang, Z., Chang, X., Zhang, M., Hu, Y., Wu, T., Wang, J., Li, B., Liu, P., Zhou, Y., Wang, A., Dong, S., Zhang, X., Gao, Q., Zhou, H., Shen, M., Wilkes, A., Miehe, G., Zhao, X., Niu, H., 2022c. Grassland changes and adaptive management on the Qinghai–Tibetan Plateau. Nat. Rev. Earth Environ. 3, 668–683. https://doi.org/10.1038/s43017-022-00330-8.

Wang, T., Huang, X., Zhang, J., Luo, D., Zheng, M., Xiang, L., Sun, M., Ren, X., Sun, Y., Zhang, S., 2023. Vegetation cover dynamics on the northeastern Qinghai-Tibet plateau since late marine isotope stage 3. Quat. Sci. Rev. 318, 108292 https://doi.org/10.1016/j.quascirev.2023.108292.

Wei, H., E, C., Zhang, J., Sun, Y., Li, Q., Hou, G., Duan, R., 2020. Climate change and anthropogenic activities in Qinghai Lake basin over the last 8500 years derived from pollen and charcoal records in an aeolian section. Catena 193, 104616. https://doi.org/10.1016/j.catena.2020.104616.

Willerslev, E., Davison, J., Moora, M., Zobel, M., Coissac, E., Edwards, M.E., Lorenzen, E. D., Vestergård, M., Gussarova, G., Haile, J., Craine, J., Gielly, L., Boessenkool, S., Epp, L.S., Pearman, P.B., Cheddadi, R., Murray, D., Bråthen, K.A., Yoccoz, N., Binney, H., Cruaud, C., Wincker, P., Goslar, T., Alsos, I.G., Bellemain, E., Brysting, A. K., Elven, R., Sønstebø, J.H., Murton, J., Sher, A., Rasmussen, M., Rønn, R., Mourier, T., Cooper, A., Austin, J., Möller, P., Froese, D., Zazula, G., Pompanon, F., Rioux, D., Niderkorn, V., Tikhonov, A., Savvinov, G., Roberts, R.G., MacPhee, R.D.E., Gilbert, M.T.P., Kjær, K.H., Orlando, L., Brochmann, C., Taberlet, P., 2014. Fifty thousand years of Arctic vegetation and megafaunal diet. Nature 506, 47–51. https://doi.org/10.1038/nature12921.

Wischnewski, J., Mischke, S., Wang, Y., Herzschuh, U., 2011. Reconstructing climate variability on the northeastern Tibetan Plateau since the last Lateglacial – a multi-proxy, dual-site approach comparing terrestrial and aquatic signals. Quat. Sci. Rev. 30, 82–97. https://doi.org/10.1016/j.quascirev.2010.10.001.

Wood, S.N., 2011. Fast stable restricted maximum likelihood and marginal likelihood estimation of semiparametric generalized linear models. J. Roy. Stat. Soc. B Stat. Methodol. 73, 3–36. https://doi.org/10.1111/j.1467-9868.2010.00749.x.

Wu, D., Zhou, A., Zhang, J., Chen, J., Li, G., Wang, Q., Chen, L., Madsen, D., Abbott, M., Cheng, B., Chen, F., 2020. Temperature-induced dry climate in basins in the northeastern Tibetan Plateau during the early to middle Holocene. Quat. Sci. Rev. 237, 106311 https://doi.org/10.1016/j.quascirev.2020.106311.

Wu, D., Ma, X., Yuan, Z., Hillman, A.L., Zhang, J., Chen, J., Zhou, A., 2022. Holocene hydroclimatic variations on the Tibetan Plateau: an isotopic perspective. Earth Sci. Rev. 233, 104169 https://doi.org/10.1016/j.earscirev.2022.104169.

Wu, D., Ma, M., Lu, Y., Guo, S., Wang, T., Ma, X., Dong, G., 2023. Out-of-phase relationship of Holocene moisture variations between the northeastern and southeastern Tibetan plateau and its societal impacts. Fundamental Research S2667325823000626. https://doi.org/10.1016/j.fmre.2023.02.014.

Yan, D., Wünnemann, B., Zhang, Y., Hartmann, K., Diekmann, B., Andersen, N., 2021. Neotectonic subsidence along the Cenozoic Kunlun Fault (Tibetan plateau). Geophys. Res. Lett. 48, e2021GL094571 https://doi.org/10.1029/2021GL094571.

Zhang, D., Xia, H., Chen, F., Li, B., Slon, V., Cheng, T., Yang, R., Jacobs, Z., Dai, Q., Massilani, D., Shen, X., Wang, J., Feng, X., Cao, P., Yang, M.A., Yao, J., Yang, J., Madsen, D.B., Han, Y., Ping, W., Liu, F., Perreault, C., Chen, X., Meyer, M., Kelso, J., Pääbo, S., Fu, Q., 2020. Denisovan DNA in late Pleistocene sediments from Baishiya Karst Cave on the Tibetan plateau. Science 370, 584–587. https://doi.org/10.1126/science.abb6320.

Zhang, N., Cao, X., Xu, Q., Huang, X., Herzschuh, U., Shen, Z., Peng, W., Liu, S., Wu, D., Wang, J., Xia, H., Zhang, D., Chen, F., 2022. Vegetation change and human-environment interactions in the Qinghai Lake Basin, northeastern Tibetan Plateau, since the last deglaciation. Catena 210, 105892. https://doi.org/10.1016/j.catena.2021.105892.

Zhang, C., Qin, D.H., Zhai, P.M., 2023a. Amplification of warming on the Tibetan plateau. Adv. Clim. Change Res. 14, 493–501. https://doi.org/10.1016/j.accre.2023.07.004.

Zhang, J., Liu, S., Qiang, M., Chen, Y., Zhang, S., Cheng, B., Pan, X., Li, Y., Huang, X., 2023b. Moisture changes in a mountain–basin system since the last deglaciation revealed by the pollen record of Genggahai Lake, northeastern Qinghai-Tibetan Plateau. Catena 225, 107046. https://doi.org/10.1016/j.catena.2023.107046.

Zhao, Y., Yu, Z., Chen, F., Ito, E., Zhao, C., 2007. Holocene vegetation and climate history at Hurleg lake in the Qaidam basin, northwest China. Rev. Palaeobot. Palynol. 145, 275–288. https://doi.org/10.1016/j.revpalbo.2006.12.002.